

https://dspace.org/

A thermodynamic analysis of photosynthesis: Quantum requirement and theoretical biomass growth rates

Kok, Heinrich Wilfrid

2012-02-14
http://hdl.handle.net/10539/11314

Downloaded from a DSpace repository. https://dspace.org/

A Thermodynamic Analysis of Photosynthesis: Quantum Requirement and Theoretical Biomass Growth Rates

Heinrich Wilfrid Kok

A dissertation submitted to the Faculty of Engineering and the Built Environment, University of the Witwatersrand, Johannesburg, in fulfillment of the requirements for the degree of Master of Engineering.

2011

Johannesburg, South Africa

Declaration

I declare that this dissertation is my own unaided work. It is being submitted for the degree of Master of Science of Engineering to the University of the Witwatersrand, Johannesburg. It has not been submitted before for any degree or examination to any other university.

.....

Heinrich Wilfrid Kok

..... day of ..... of the year .....

Abstract

Interest in photosynthesis continues to increase with a global focus on developing alternative fuel sources such as biofuels. It is the various forms of biomass that provide the raw materials for the production of biofuels such as bioethanol and biodiesel. The vast majority of these materials are grown by the photosynthesis process. Developing a mathematical model of the process allows for a clearer understanding of what limits and propels the process, and what this reaction might be capable of in terms of biomass growth on an industrial scale.

The primary driving force of photosynthesis, solar energy, is a crucial aspect of this model. Relating the amount of light to organism growth is done by exploring the concept of quantum requirement, which is essentially the amount of photons needed to drive the photosynthesis reaction. The theoretical quantum requirement calculated is dependent on the wavelength of incoming photons in the photosynthetically active radiation (PAR) spectrum, and varies between 9.94 moles of photons per mole of biomass (approximated as glucose) at 400nm, and 17.8 moles of photons per mole of biomass at 700 nm. Measured, experimental values of quantum requirement from the literature considered here average a value of 61.7 moles of photons per mole of biomass required.

The conclusion is that the theoretical lower limit of operation, which is therefore the absolute minimum quantum requirement, occurs when the photosynthesis process operates reversibly. It is suggested that the large difference between theoretical and measured quantum requirement values may indicate that the photosynthesis process is irreversible in nature. By the model developed, two other observations of interest are made: photon entropy has little effect on the calculated quantum requirement; heat must be rejected from the process, and increases in magnitude with increasing irreversibility.

In the final chapter, the theoretical model for quantum requirement is utilised in conjunction with spectral irradiance data to obtain estimates of theoretical photosynthetic growth rates. With a reversible photosynthetic process, a growth rate of 81.0 $\mathrm{g/m^2}$.hr of biomass would be possible if all light energy in the PAR spectrum were absorbable. Applying the absorption capabilities of a commonly-occurring pigment such as chlorophyll *a*, this theoretical growth rate is reduced to 20.0$\mathrm{g/m^2}$.hr, to indicate the light saturation and absorption-limited effect of a plant's cell biology.

Both values are still largely above experimentally determined growth rates from literature. These discrepancies are discussed with focus on relevant enzymes and proteins in the light-dependent and light-independent reactions of

photosynthesis that limit its kinetics and efficiency. The importance of calculating maximum possible biomass growth rates is that they, in essence, set the upper limits on biomass production in our environment. With this knowledge, large-scale estimates can be made, and improved efficiencies can be targeted and measured against the ideal, theoretical case.

Acknowledgements

I wish to thank and acknowledge the following people:

- My parents, Hennie and Sue Kok, for there constant support and interest.
- Nik Felbab, for his excellent friendship, encouragement and inspiration.
- Michelle Low, for her contributions to and insight into the subject matter of Chapter 2 of this dissertation, as well as for all her work and assistance on the posters and presentations that we prepared together during the last two years.
- Professors Diane Hildebrant and David Glasser, for their supervision, advice and help throughout this project.
- David Ming, Michelle Low, Graham Bathgate, Antony Higginson, Rosalind Dos Santos and Craig Griffiths for their friendship during my time as an undergraduate and postgraduate at Wits.
- COMPS (Centre of Material and Process Synthesis), for their financial support.

Contents

Declaration **1**

Abstract **2**

Acknowledgements **4**

Contents **5**

List of Figures **8**

List of Tables **11**

List of Frequently Used Symbols **12**

1 Introduction to Photosynthesis **14**

1.1 Background and Motivation 14

1.1.1 The relation between photosynthesis and biofuels 14

1.1.2 Atmospheric carbon dioxide mitigation 15

1.2 Aims and Objectives 16

1.3 Literature Review 17

1.3.1 The basics of photosynthesis 17

1.3.1.1 The overall equation 17

1.3.1.2 Light-dependent reactions 19

1.3.1.3 Light-independent reactions 22

1.3.1.4 Light absorption 23

1.3.2 The relevance of algae 26

1.3.3 Characteristics of light 27

1.3.3.1 Energy 27

1.3.3.2 Spectral irradiance 28

1.3.3.3 Entropy 29

1.3.4 Quantum requirement 30

1.3.5 Photosynthetic efficiency and growth rates 32

2 Calculating the Quantum Requirement 35

2.1 Method of Approach 35
2.1.1 Mass and energy balances 36
2.1.2 Entropy balance 39
2.1.3 Gibbs free energy definitions 42
2.2 Results of the Analysis 44
2.2.1 Zero heat scenario 44
2.2.2 Reversible, zero photon entropy scenario 45
2.2.3 Reversible, finite photon entropy scenario 46
2.2.4 Increasing irreversibility 47
2.2.5 Heat rejection and irreversibility 49
2.3 Discussion and Conclusions 52
2.3.1 Photon entropy 52
2.3.2 Limits of operation 52
2.4 Further Analysis: Heat Rejection Feasibility 54
2.4.1 Macroscopic heat rejection 54
2.4.2 Microscopic model of heat rejection per time 56
2.4.3 Results and discussion 58

3 Theoretical Biomass Growth Rates 60

3.1 Introduction and Approach 60
3.2 Reversible Process 61
3.2.1 Total incident light 61
3.2.2 Total absorbable light 64
3.3 Irreversible Process 65
3.3.1 Total incident light 65
3.3.2 Total absorbable light 65
3.4 Photosynthetic Efficiency 66
3.5 Results 67
3.6 Discussion 72

4 Conclusions and Recommendations 75

Bibliography 77

A Linking Irreversibility and Heat Rejection 83

B Heat Transfer Profile for a Microalgae Species **85**
B.1 Introduction 85
B.2 Heat transfer over the cell 87
B.3 Heat transfer over the water film 89

List of Figures

1.3.1 The relationship between oxygen evolution and light intensity, as demonstrated by Melis (2009) for a species of microalgae. The rate of oxygen evolution is given as the number of moles of oxygen produced per mole of chlorophyll per second. The light intensity, or irradiance, is described as the number of photons received per area per second. 24
1.3.2 Percentage absorbance of incident light for chlorophyll *a* in the photosynthetically active radiation spectrum (Whitmarsh and Govindjee, 1999). Absorption peaks are observed at approximately 440 nm and 680 nm, which are the blue and red light regions, respectively. These areas are also referred to as the action spectrum for the photosynthesis reaction. 25
1.3.3 Spectral irradiance of the sun. 28

2.1.1 Diagram of the "black-box" approach, which considers the overall flows of mass, energy and entropy. The inner processes are not dealt with. 35
2.1.2 The mass balance for the photosynthesis process, with phases of the components indicated. 36
2.1.3 The energy balance for the photosynthesis process. 37
2.1.4 The entropy balance for the photosynthesis process. 40
2.2.1 Minimum quantum requirement for glucose synthesis from energy balance corresponding with the scenario of zero heat (Q = 0), compared to the average value quoted by literature. 45
2.2.2 Minimum quantum requirement for reversible glucose synthesis with zero (Gudkov, 1998) and finite (Kirwan, 2004) values of photon entropy, compared to the average quantum requirement from literature. 46

2.2.3 Minimum quantum requirement values for different and increasing values of internal entropy generated per mole of reaction (S_{gen}) of the process, in comparison with the average quantum requirement from literature. 48
2.2.4 Contour plot of the heat rejected by the system (Q) as a function of internal entropy generated per mole of reaction (S_{gen}) for the finite photon entropy scenario. The dashed line indicates the process at reversible conditions, where $S_{\text{gen}} = 0$. Process irreversibility increases as one moves above this line. The contours for heat rejection at reversible conditions for photons of 400 nm and 700 nm occur and are shown with 166 kJ/mol and 238 kJ/mol, respectively. 49
2.2.5 Contour plot of the heat rejected by the system (Q) as a function of internal entropy generated per mole of reaction (S_{gen}) for the finite photon entropy scenario. The graph is an extended version of figure 2.2.4, showing now the theoretical negative spectrum of photon wavelength. The dashed line indicates the process at reversible conditions, where $S_{\text{gen}} = 0$. Process irreversibility increases as one moves above this line. The intersection of contour $Q = 0$ with $S_{\text{gen}} = 0$ can be seen at a wavelength of -307 nm. . 50
2.2.6 Heat rejected by the system (Q) as a function of internal entropy generated per mole of reaction (S_{gen}) for the zero photon entropy scenario. The dashed line indicates the process at reversible conditions, where $S_{\text{gen}} = 0$. Process irreversibility increases as one moves right of this line. 51
2.4.1 Heat rejected by the photosynthesis system utilising the average literature quantum requirement of 61.7 moles of photons at different wavelengths in the photosynthetically active radiation spectrum (PAR). 55
2.4.2 Heat transfer over a simplified, spherical algal cell. Heat transfer occurs in the direction outwards from the centre of the cell, as well as over the surface of the cell to the bulk fluid (water) over a film of the fluid. 56

2.4.3 Inner core temperature of a microalgal cell with increasing radius size resulting from heat rejection. The ambient temperature is chosen to be 25 °C. Typical algae cells will range with radii between 1 and 6 microns (Graham and Wilcox, 2000). The heat rejected is compared for case of the average literature quantum requirement (the irreversible process) and for the quantum requirement from the reversible process. The incoming photons to the organism are of wavelength 680 nm, a common absorbance peak for chlorophyll *a*. 59

3.2.1 Measured solar irradiance ($W/m^2.nm$), shown in figure 3.2.1a, and equivalent incoming photon density (mol photons/m^2.s.nm), shown in figure 3.2.1b, at sea level with the photosynthetically active radiation (PAR) limits at 400 nm and 700 nm indicated by vertical dashed lines. 63

B.1.1 Heat transfer over a simplified, spherical algal cell. Heat transfer occurs in the direction outwards from the centre of the cell, as well as over the surface of the cell to the bulk fluid (water) over a film of the fluid. 86

List of Tables

1.3.1 Comparative values of photosynthesis quantum requirements from literature. 32

3.5.1 Summary of theoretical and literature-based rates of carbon dioxide uptake, oxygen evolution, and maximum biomass generation. The reversible rates utilise the theoretical quantum requirement in the minimum limit of operation scenario, while the irreversible rates utilise the average literature quantum requirement. The measured rates are given for oxygen evolution in the case of Doucha et al. (2005), and for carbon dioxide uptake by Moss (1967) and Goudriaan and van Laar (1994). The stoichiometrically equivalent biomass rates are the maximum possible, but not necessarily realistically attainable, due to reaction kinetic differences and inefficiencies. 69

3.5.2 Photosynthetic efficiences calculated from the biomass growth rates in table 3.5.1, and based upon the total amount of light received in the photosynthetically active radiation spectrum of 400 nm to 700 nm. 70

List of Frequently Used Symbols

$\Delta G^{\circ}_{\mathrm{f,i}}$ Standard Gibbs free energy of formation of substance i (kJ/mol)

$\Delta G^{\circ}_{\mathrm{rxn}}$ Gibbs free energy of reaction (kJ/mol)

$\Delta H^{\circ}_{\mathrm{f,i}}$ Standard enthalpy of formation of substance i (kJ/mol)

$\Delta H^{\circ}_{\mathrm{rxn}}$ Enthalpy of reaction (kJ/mol)

$\dot{N}_{\mathrm{glucose}}$ Glucose or approximated biomass generation rate ($\mathrm{g/m^2.hr}$)

$\hat{S}_{\mathrm{photon}}$ Entropy of a photon (J/K)

λ Photon wavelength (nm)

$\mathrm{QR_i}$ Quantum requirement of substance i (mol photons/mol substance)

c Speed of light (2.998×10^8 m/s)

h Planck's constant (6.626×10^{-34} J.s)

I Spectral or solar irradiance ($\mathrm{W/m^2.nm}$)

k Boltzmann's constant (1.381×10^{-23} J/K)

N_{A} Avogadro's number (6.022×10^{23} particles/mol)

Q Amount of energy rejected to the surroundings as heat per mole of reaction (kJ/mol)

q Rate of heat rejection from the system to the surroundings (W)

r_{i} Reaction rate of substance i ($\mathrm{mol/m^2.s}$)

S_{gen} Internal entropy generated within the process (kJ/mol.K)

T_{o} Ambient temperature (25 °C)

Chapter 1

Introduction to Photosynthesis

1.1 Background and Motivation

1.1.1 The relation between photosynthesis and biofuels

The importance of the photosynthesis reaction in nature cannot be understated; the usage of sunlight to form simple, organic compounds from water and carbon dioxide, whilst releasing oxygen to the environment, is an essential life-supporting mechanism. Indeed, a co-dependent and cyclic relationship between autotrophs and heterotrophs exists; this is directly facilitated by photosynthetic activity (Bryant and Frigaard, 2006).

Increased global awareness of the earth's rapidly depleting fossil fuels has led to a growing demand for reduced usage of these fuels. In turn, investigations have begun as to how the world's energy requirements can be satisfactorily supplied, and possibly replaced, by the implementation of alternative fuels. Biofuels currently offer a viable opportunity to accommodate at least part of this fuel usage shift. Biodiesel and bioethanol, in particular, have been identified as appealing substitutes to fulfill transportation fuel demands (Demirbas, 2009).

The raw materials utilised in the production of biofuels are varied; crops (Ragauskas et al., 2007), algae (Chisti, 2007), and other organic matter, which together constitute the term "biomass", are all potential feedstocks in the conversion of biomass to fuels. All forms of biomass must be grown and therefore effectively produced from the photosynthesis process. The photosynthesis reaction utilises the energy provided by the sun to convert carbon dioxide and water into more complex organic substances and, in turn, trap or install the energy received from the sun into these molecules.

This energy is then later transferred to biofuels, which are evolved by appropriate chemical processes. So, not only is the photosynthesis process important to the general functioning of our planet, but it forms an integral part in the investigation and analysis of fuels production from biomass, since a very large amount of carbon dioxide is converted to biomass each year by this process (Field et al., 1998).

The benefit of solar energy is that it is technically "free" and long-lasting; the energy of the sun is provided to the earth in the form of photons and is received by land and sea areas. This will continue to occur with the lifespan of the sun. However, the choice of utilising this seemingly unlimited energy, with effective research and development, rests with society.

1.1.2 Atmospheric carbon dioxide mitigation

The issue of finding alternative fuel sources is not the only concern at stake. The worries of global warming and the causative insulating effect of greenhouse gases, such as carbon dioxide, on the earth's atmosphere have developed substantially in the last few years (Karnaukhov, 2001). The amount of carbon dioxide present in the earth's atmosphere has increased over recent centuries as a result of increased fossil fuel burning and deforestation. A proportional relationship with population growth is evident in this regard (Karube et al., 1992).

Thus, it is necessary to investigate fuel production processes that involve minimal carbon dioxide emissions, and even possibly to the extent of involving or promoting carbon dioxide sequestration.

A direct advantage of photosynthesis is that of its ability to capture carbon dioxide, and this is plainly apparent in the nature of the chemical reaction. The uptake of carbon dioxide and release of oxygen by photosynthetic organisms is one method of reducing the amount of carbon dioxide in the atmosphere. A combination of lowering industry carbon dioxide outputs by taxation, better industrial process designs, and maximising global photosynthetic processes could assist in remedying the global warming problem.

In summary, the aforementioned problems, namely that of society's current dependence on non-renewable energy sources, and that of the excess, atmospheric carbon dioxide's global warming effect on the earth, are both approached and conceptually rectified with photosynthesis. In a world running low on fossil fuels that cannot be quickly replenished, hope lies with usage of the sun's energy for the creation of biomass from photosynthesis, and the sub-

sequent creation of biofuels to satisfy a portion of humanity's energy demands.

The role of the engineer in this sphere, and indeed what this dissertation intends to accomplish, is to explore and understand the fundamentals of photosynthesis from a thermodynamic standpoint. This type of understanding allows a model to be developed, which can essentially provide the theoretical constraints of how the reaction or process can proceed. On a macroscopic scale, this model can be applied to estimating the generation of biomass. The pursuit of this latter task is important, as these estimations can assist in providing the biofuels industry with information about the quantities of biomass that can be produced as raw material feedstock for biofuels creation.

1.2 Aims and Objectives

The primary aim of this work is to be able to mathematically model the photosynthesis reaction as a function of photon input, or energy received from the sun. This determination of how much photon energy is required to allow the reaction to occur is an important one, as Govindjee (1999) suggests that this allows an understanding of the efficiency of energy storage in photosynthesis. Though this analysis is theoretical, there is an abundance of literature measuring experimental values of photon requirements for the photosynthesis reaction. With this literature available, comparisons can be made, and discussion of any discrepancies initiated. This concept is referred to as the quantum requirement of photosynthesis, and will be examined in greater detail in section 1.3.4.

Ogbonna et al. (1995) emphasises the point that mathematical modelling is extremely useful and necessary in the consideration of bioprocesses and understanding them. This modelling shall involve thermodynamic examinations of the photosynthesis process and definitions of the system at hand. In addition to this, the effect and concept of photon wavelength will be investigated, as it relates directly to energy input.

Petela (2008) discusses and highlights some important points about a thermodynamic analysis of a system. Of these, eventual optimisation of the process is a primary goal, and this is achieved by understanding what variables and primary influences affect the functioning of it. Establishing the limits or bounds of operations gives clear definition to the minimum and maximum values of such variables. Likewise, in this analysis, it is the hope that the photosynthesis process and system can be optimised.

An additional or secondary objective is to consider the available solar energy from the sun, so that the model developed can be combined to calculate the organic matter or biomass produced by photosynthesis per period of time and land area. Essentially, if the photosynthesis process can be quantified, then absolute theoretical estimates and limits regarding the conversion of light energy into chemical energy and plant mass can be established (Beadle and Long, 1985).

1.3 Literature Review

1.3.1 The basics of photosynthesis

1.3.1.1 The overall equation

Photosynthesis is the biological process of converting carbon dioxide and water into oxygen and organic materials such as sugars and carbohydrates with the usage of light energy. Different plant and algae species use similar or even identical photosynthetic pathways that convert this light energy into a form of chemical energy, retained by the plant or algae in its cells (Björkman and Demmig, 1987). The generalised equation or mass balance for the physical components of the photosynthesis reaction is shown here by equation 1.3.1:

$$n\mathrm{CO_2} + n\mathrm{H_2O} \longrightarrow (\mathrm{CH_2O})_n + n\mathrm{O_2} \tag{1.3.1}$$

Since the photosynthesis process is by its nature a chemical work-requiring process, the light energy received from photons acts as a supply to this requirement. Without this input, the synthesis cannot occur; phototropic organisms can only grow and exist if a supply of light energy is available to them.

Typically, in photosynthesis equation analysis, glucose is assigned as the primary organic product to represent the growth of organic matter. Glucose is a sugar molecule and an important source of energy in plants, which ultimately contributes to the formation of other products including cellulose, a main constituent in plant and alga cells. The photosynthesis reaction for the production of glucose is provided here in equation 1.3.2:

$$6\mathrm{CO_2} + 6\mathrm{H_2O} \longrightarrow \mathrm{C_6H_{12}O_6} + 6\mathrm{O_2} \tag{1.3.2}$$

A thermodynamic analysis of any system requires the usage of mass, enthalpy and entropy balances. In turn, this requires enthalpy and Gibbs free

energy formation data, or even entropy formation data, for each reactant and product. The advantage of glucose as the chosen product for the synthesis analysis is revealed in the availability of both its enthalpy and Gibbs free energy formation data. It should be noted that this would be difficult to accomplish for an alternative product, such as cellulose or starch, where such data is not available. This reasoning, coupled with glucose being a major and common product of photosynthesis, justifies the selection of glucose as the chosen photosynthesis product in the approaching analysis.

However, even with this data available, there is the issue of ambiguity of phase of the organic product, glucose. On a microscopic scale, the glucose formed in the reaction can either be formed as a solid product or as a dissolved product in surrounding, excess water – the latter a possibility to consider due to the high solubility of glucose in water. As a result, it is difficult to ascertain exactly in which phase the glucose will be produced. Fortunately, with this question of phase in mind, enthalpy of formation and Gibbs free energy of formation data is available for both phases, and so comparisons between the two phases can be drawn. The enthalpy of formation and Gibbs free energy of formation values for glucose in the aqueous phase are sourced from Alberty (1998):

$$\Delta H^{\circ}_{\mathrm{f,C_6H_{12}O_6,aqueous}} = -1262.19\,\mathrm{kJ/mol}$$

$$\Delta G^{\circ}_{\mathrm{f,C_6H_{12}O_6,aqueous}} = -915.90\,\mathrm{kJ/mol}$$

These can be compared with enthalpy of formation and Gibbs free energy of formation values for glucose in the solid phase, which are sourced from Brown et al. (2002):

$$\Delta H^{\circ}_{\mathrm{f,C_6H_{12}O_6,solid}} = -1271\,\mathrm{kJ/mol}$$

$$\Delta G^{\circ}_{\mathrm{f,C_6H_{12}O_6,solid}} = -909\,\mathrm{kJ/mol}$$

It can be observed that the differences in values between the enthalpy of formation and Gibbs free energy of formation for each phase are noticeably small. This would imply that the enthalpy change and Gibbs free energy change between these two phases – in essence, the process of solvation – will both be very minor. Indeed, this may have bearing on the high solubility of glucose in water. However, this is not the discussion at hand.

What is important, is that the choice of phase will have little impact on thermodynamic calculations such as those performed in an energy balance, considering that the enthalpy of formation of glucose in the solid phase is approximately equal to the enthalpy of formation of glucose in the aqueous

phase. The same can be said of the choice of phase and the Gibbs free energy of formation of glucose, and hence its involvement in an entropy or Gibbs free energy balance. Following this conclusion, it should be noted that the values for the enthalpy of formation and Gibbs free energy of formation of glucose that are used in all calculations of this dissertation are, by choice, those provided by Alberty (1998).

1.3.1.2 Light-dependent reactions

Attention must now be drawn to the inner workings of the photosynthesis process. Although the focus in this dissertation is the application of engineering principles to photosynthesis as an overall process, having knowledge of some of its intricacies and many interlinked reactions may assist in discussing and reconciling the results of the analysis with the results from experimental literature.

The inner cell workings of the photosynthetic process are complex and detailed, and there are several reactions that contribute and stem from one another to eventually represent the overall reactions shown in equations 1.3.1 and 1.3.2. Division between two types or sets of reactions in the photosynthesis process is usually made: light-dependent (photo) reactions, are directly influenced by the light or photon input into the system; light-independent (non-photo) reactions occur without the direct stimulation of light or photon input (Petela, 2008).

The light-dependent reactions are to be explained first, as the products of these reactions provide the light-independent reactions with energy-rich molecules to proceed. Indeed, two of the most important of these molecules are ATP (adenosine triphosphate) and NADPH (nicotinamide adenine dinucleotide phosphate), which are formed within a cycle and utilised in the light-independent reactions. The light-dependent reactions occur in specialised areas of a plant's cells, called chloroplasts. In turn, these chloroplasts house chlorophyll molecules, which are central to the photosynthetic process as photoreceptors, absorbing light or photon energy, and indeed initiating a consequent chain of events that will convert light energy to chemical energy (Beadle and Long, 1985). Carotenoids perform a very similar role, and are available depending on the plant type.

Each species of plant or algae tend to possess a variety and combination of different types of chlorophyll molecules in the chloroplast organelles of their cells. Chlorophyll a and chlorophyll b are two of the most common types of

chlorophyll molecules – the former being the most common – found in plants and algae (Nabors, 2004). The light that these molecules are capable of absorbing corresponds to the spectrum of photosynthetically active radiation (PAR). This spectrum encompasses photons from approximately 400 nm to 700 nm in wavelength (Fragata and Viruvuru, 2008), which is a slightly shorter than the range of visible light, 380 nm to 780 nm (Petela, 2008). Plants and algae tend to be able to absorb light in the red and blue colour spectra particularly well, thus defining their action spectra, as a result of the nature and function of the chlorophyll molecules they contain in their chloroplasts. These absorption peaks occur for chlorophyll *a* at about 430 nm and 680 nm (Berg et al., 2002).

Within these chloroplasts, a photosynthetic or thykaloid membrane is in place, which contains the necessary proteins for the light-dependent reactions. Moving outside of this membrane, but still within the chloroplast, other proteins and enzymes are available for the carbon reduction or light-independent reactions (Whitmarsh and Govindjee, 1999). This area is known as chloroplast stroma, whereas the interior of the membrane is referred to as the thykaloid lumen. Inside the membrane, two crucial reaction centres, or light-harvesting complexes, operating in series are available: P680 and P700, also known as Photosystem II and Photosystem I, respectively. Each protein complex is surrounded by a collection of chlorophyll (or carotenoid) molecules that collect photons. The starting point of the light-dependent reactions involves the photoexcitation of electrons within P680 by received photons collected by the chlorophyll molecules (Jones and Fyfe, 2004). With the heightened energy state of these electrons, the P680 transfers the electrons on to another complex, pheophytin. The transferred electrons from P680 are replaced by the oxidation of surrounding water molecules (Shinkarev, 2003). In the process of oxidising the water, oxygen molecules are released:

$$\mathrm{H_2O} \rightarrow \frac{1}{2}\mathrm{O_2} + 2\mathrm{H^+} + 2\mathrm{e^-}$$

This is a significant reaction, and the P680 protein complex is thus responsible for the release of oxygen into the atmosphere. The electrons transferred to the pheophytin continue down an electron transport chain – also known as the Z-scheme – through various molecules, acting as vehicles, to the protein complex Cytochrome c6f, and then onto the second reaction centre, P700 (Govindjee and Govindjee, 2000). It is not the intention of this dissertation to describe each and every event in this transport chain, as the process is extremely detailed and intricate. However, relevant points will be drawn into

discussion when considering limited reactions and constrictions in the process, as these will be relevant to theoretical and measured growth rate comparison.

One such point to be considered occurs at the protein complex Cytochrome c6f. Plastoquinone, one of the aforementioned molecules that works as a vehicle to transport electrons, moves cyclically between P680 and Cytochrome c6f to transfer electrons in a reduced and oxidised state. The reduced form of plastoquinone will bind to certain sites on the Cytochrome c6f complex, where oxidation of it by a FeS molecule will occur in order to move the electron along the electron transport chain, or Z-scheme. According to Govindjee and Govindjee (2000), this process occurs in a matter of milliseconds, whereas photoexcitation in the reaction centres P680 and P700 is in the rate region of picoseconds. Thus, the overall rate of the light-dependent reactions could be limited by this particular action. As further information of interest, the oxidised form of plastoquinone would then return to the P680 site to continue its cycle by receiving another electron and returning to its reduced form.

Continuing down the electron transport chain, the electron will reach P700. Here the phenomenon of photoexcitation is again observed, with the reaction centre receiving energy from incoming photons, and continuing the electron gradient and transfer direction towards the enzyme ferrodoxin-NADP reductase. This enzyme allows the reduction of NADP molecules on the stroma side of the membrane into NADPH molecules by combining protons within the stroma with electrons from P700.

Whilst this accounts for the production of NADPH, the synthesis of ATP must also be explained here. With the release of protons from the oxidisation of water on the lumen side, as well as the drawing of protons across the thykaloid membrane during the reduction and oxidation of plastoquinone between P680 and the Cytochrome c6f complex, a proton motive force or gradient is formed across the thykaloid membrane (Whitmarsh and Govindjee, 1999). Once in the lumen, these protons move towards the ATP-synthase enzyme. It is here then where ADP (adenosine diphosphate) on the stroma side binds to a site on the ATP-synthase enzyme to form ATP, in combination with the proton that crosses the membrane from the lumen to the stroma side. The ATP is released on the stroma side of the membrane, where it is used in the light-independent reactions.

1.3.1.3 Light-independent reactions

As can be seen, the production of ATP and NADPH in the stroma is directly reliant on the functioning and creation of an electron transport chain by the photosynthetic reaction centres P680 and P700 in the thykaloid lumen. Again, as with the light-dependent reactions, the light-independent reactions are numerous and complex, and will not be described here in their totality. However, there are several focal points of interest. The basic functioning of the light-independent reactions occurs on the stroma side of the thykaloid membrane. The overall process of converting carbon dioxide from the atmosphere to carbohydrates in the organism is called the Calvin cycle.

Carbon dioxide is absorbed by the Ribulose 1,5-biphosphate molecule and then broken into two 3-phosphoglycerate molecules. This process is catalyzed by a key enzyme in the process, Rubisco, and the carbon dioxide must attach or bind itself to appropriate sites on the Rubisco protein during this reaction (Taiz and Zeiger, 2010). The ATP and NADPH molecules created from the light-dependent reactions are oxidised back to their states of ADP and NADP, respectively, at points during this cycle. However, in doing so, they donate energy by reducing the 3-phosphoglycerate molecules along a pathway to eventually form triosephosphate, which is essentially a building block to greater sized carbon or sugar molecules such as glucose, starch, cellulose and other sugars (Whitmarsh and Govindjee, 1999).

These sugars are utilised as structural materials for the plant, as well as for cellular respiration, which is the mechanism that allows organisms to obtain energy by effectively consuming them (Beadle and Long, 1985). In a sense, cellular respiration is the reverse reaction of photosynthesis, but it does not involve light input or output. The ADP and NADP molecules are returned to the aforementioned Z-scheme electron transport chain where they will be reduced again by the light-dependent reactions back to ATP and NADPH, respectively.

It is not entirely true to say that the light-independent reactions are entirely light-independent, as they would not be able to proceed without sufficient ATP and NADPH, which are created by the light-dependent reactions. Indeed, at night, when very little to no light is available, oxygen evolution from the light-dependent reactions halts (Melis, 2009). Subsequently, so does production of ATP and NADPH, without which the light-independent processes of carbon fixation and carbohydrate formation cannot occur, thus explaining the lack of nocturnal plant growth. What is true to say, however, is that the light

intensity does not influence the rate of function of the some of the enzymes of the carbon fixation and reduction processes, to which must attention must now be drawn to.

A major consideration to be made is that of the enzyme Rubisco. As mentioned, Rubisco is essential as it binds carbon dioxide molecules with Ribulose 1,5-biphosphate molecules in the process of carbon reduction. One of the complex aspects of Rubisco is the issue of specificity of reaction, since the enzyme is capable of binding carbon dioxide molecules for the carbon reduction, as well as oxygen molecules for photorespiration. Indeed, this reveals two competing reactions. Photorespiration is viewed to be energy-wasting, and inhibits carbon fixation, which ultimately slows structural development and plant growth (Tcherkez et al., 2006). Atmospheric environments with high carbon dioxide concentration and low oxygen concentration will tend to promote carbon fixation (Parry et al., 2003), but increasing carbon dioxide concentration can only be successful to a point, as further increasing it will result in the poisoning of the organism, as observed in some species of algae (Myers, 1953).

The enzyme has also been targeted as a severely rate-limiting enzyme in the overall photosynthetic process, decreasing its total efficiency, and thus resulting in a call for genetic modification and alteration of the enzyme in order to improve its performance (Parry et al., 2003; Andrews and Whitney, 2003; Whitney and Andrews, 2001). Aside from reaction specificity, the main area of problem with Rubisco is in its slow rate of binding molecules to its available sites in order to catalyse carbon fixation; the enzyme is able to handle only a few interactions per second (Tcherkez et al., 2006). When compared with the light-dependent reaction rates that range between one interaction per picosecond to reaction per millisecond (Govindjee and Govindjee, 2000), this is a large difference. To conclude, the light-dependent reactions and light-independent reactions occur at different rates, but it is the light-independent reactions that limit the overall rate of the photosynthesis process.

1.3.1.4 Light absorption

As mentioned, the evolution of oxygen is a direct consequence of the light-dependent reaction. Melis (2009) offers insight into this relationship between light intensity and the rate of oxygen evolution, as demonstrated in Figure 1.3.1. With zero light intensity, a negative rate of oxygen evolution can be observed as a result of cellular respiration. Cellular respiration can be thought of as the opposite process of photosynthesis; sugars are combusted (thus con-

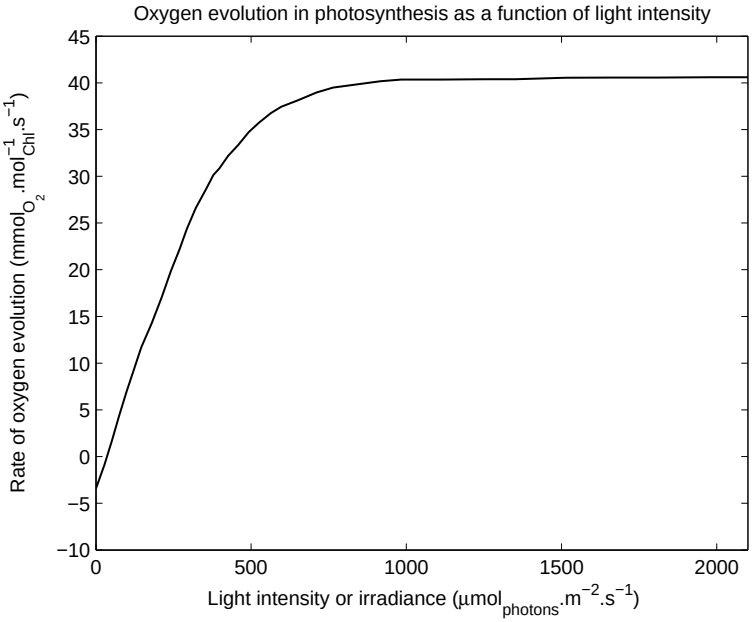


Figure 1.3.1: The relationship between oxygen evolution and light intensity, as demonstrated by Melis (2009) for a species of microalgae. The rate of oxygen evolution is given as the number of moles of oxygen produced per mole of chlorophyll per second. The light intensity, or irradiance, is described as the number of photons received per area per second.

suming oxygen) to provide energy to other areas of the cells of a plant or algae. Returning to the graph, the rate of oxygen evolution increases with light intensity. However, at higher intensity levels, the rate of oxygen evolution tends to plateau and become constant, indicating saturation.

The significance of this plateau is that the maximum amount of photon energy absorbed per time has been reached; all additional and unabsorbed light received cannot be utilised, and is rejected as heat or reflected by the organism. To establish why this saturation effect occurs, the details of the light-dependent and light-independent reactions from sections 1.3.1.2 and 1.3.1.3 must be considered.

The point made by Govindjee and Govindjee (2000) regarding the slow binding plastoquinone to the Cytochrome c6f complex is a bottleneck of concern. Examining the light-independent reactions, the primary bottleneck is revealed to be the Rubisco enzyme, with its particularly slow enzyme rate (Tcherkez et al., 2006). Melis (2009) confirms both these phenomena to be causes of the light saturation effect. The relative rate of Rubisco when compared to the activity of the Cytochrome c6f complex is slower, and so ultimately this is the overall rate-limiting step.

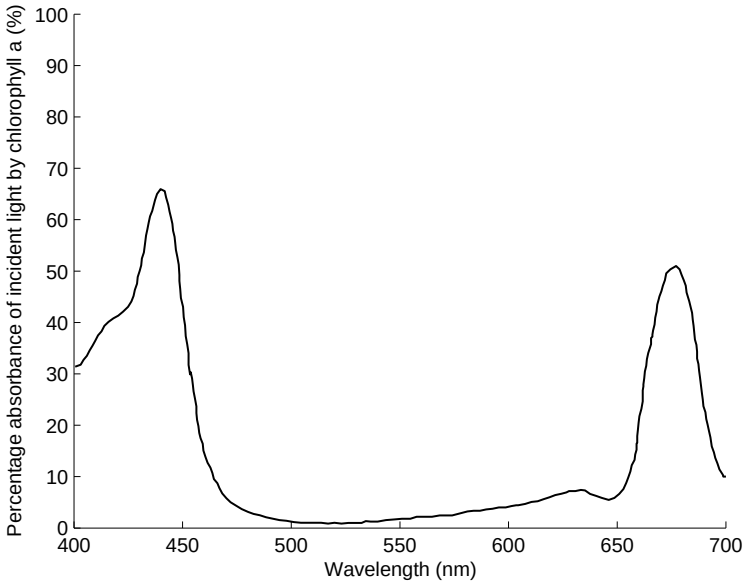


Figure 1.3.2: Percentage absorbance of incident light for chlorophyll a in the photosynthetically active radiation spectrum (Whitmarsh and Govindjee, 1999). Absorption peaks are observed at approximately 440 nm and 680 nm, which are the blue and red light regions, respectively. These areas are also referred to as the action spectrum for the photosynthesis reaction.

While the absorption of light energy has been examined from a quantitative viewpoint in terms of number of photons, the absorption ability of photosynthetic organisms must be considered from a qualitative perspective too. This refers to the concept that photons of every wavelength in the photosynthetically active radiation spectrum are not absorbed by light-reaction centres P680 and P700 equally. Whitmarsh and Govindjee (1999) provide a percentage absorbance curve in figure 1.3.2 for the chlorophyll a pigment.

Percentage absorbance can be defined in a simple manner as:

$$A_\lambda = \frac{\text{Total light absorbed for } \lambda}{\text{Total light received for } \lambda} \times 100$$

A pigment's absorption capabilities dictate ultimately how much light energy can be converted to chemical energy. The usefulness of this percentage absorbance curve will be revealed in the calculation of theoretical growth rates, where one is able to compare such growth rates based on the total light an organism might receive versus the realistically absorbable light. The latter is expected to be less than the former, and the difference between the two will be considered in chapter 3.

1.3.2 The relevance of algae

The relevance and value of algae in contemporary industry and society is at a highpoint with its potential in the biofuel and food markets. In the biofuel industry it is possible to produce biodiesel, biobutanol, biogasoline and several other fuels from algae. Biodiesel currently ranks as the most worthy of consideration for replacing current automobile fuels, according to a report by the US Department of Energy Aquatic Species Program (2006). It is noteworthy that up to 60% of the biomass of algae grown can be extracted as oils for the production of biodiesel, as stated by the Australian research group SARDI Aquatic Sciences (2008).

With regard to use as a food source or supplement, algae are protein-rich, easily digestible and highly nutritious, making them excellent foods for consideration in developing countries or countries where low-cost food is in demand (Burlew, 1953). The use of microalgae extends even to having potential in pharmaceutical development (Melis, 2009).

The main reason, however, for including algae in this discussion is for examination of their promising capabilities in atmospheric carbon dioxide mitigation, a global need observed in section 1.1.2. An overview of industrial processes and opportunities that incorporate this approach seems appropriate to further promote this study and the objectives of it.

Algae possess simple and, quite often, uniform cellular structures, which therefore allow estimation and monitoring of such growth to be more easily modelled and controlled. Spoehr (1953) suggests that the composition of a unicellular alga such as the *Chlorella* species can be varied by controlling the growth conditions and nutrients available to yield a product of desired composition. Controlling growth conditions also allows algae to be grown throughout the year if at the correct temperature range, unlike many seasonal crops (Doucha et al., 2005). In addition, many algal species, with types of microalgae in particular, have the ability to grow biomass at higher photosynthesis rates than other plant forms of increasing complexity. With these appealing growth rates, algae appear as a suitable candidate for large-scale biomass growth (Karube et al., 1992).

Another advantage that microalgae have is that they are able to grow and function under high carbon dioxide concentrations. Since this allows biomass to be grown in gases of high carbon dioxide concentration, industrial opportunities are available for such utilisation; flue gases from factories and power plants can be used as feed gases to microalgal growth facilities (Karube et al.,

1992).

Indeed, it is such factories and power plants that are responsible for the majority of annual carbon dioxide output into the atmosphere, and this is a direct method of capturing that carbon dioxide. Doucha et al. (2005) mention that an added benefit of this process is that it allows biomass to be grown cheaply, since the feed consists of by-product flue gases from other operations, and this eliminates the cost of purchasing carbon dioxide feed from a source. Minerals, nutrients and water costs will, however, have to be funded and the materials sourced.

Debate in regard to the procedure and equipment that algae should be grown is apparent; algal ponds and photobioreactors currently represent two of the main methods for large-scale algae growth (Doucha et al., 2005; Jeong et al., 2003; Karube et al., 1992). Regardless of the advantages and disadvantages of each growth technique, properly developed methods do exist to assist in the mitigation of atmospheric carbon dioxide on a large-scale.

1.3.3 Characteristics of light

1.3.3.1 Energy

Photons are the units or constituent components of light that are produced from a black body, such as the sun, and received by the earth. Photons exist as both particles and waves, and therefore occupy space and have inherent wavelength; the latter property allows the energy contained in light or photons to be quantified. The energy of a photon, $\hat{E}_{\text{photon}}$, is inversely proportional to its wavelength. Work published by Planck (1901) allows the calculation of the energy of a photon from the sun as a function of its wavelength λ:

$$\hat{E}_{\text{photon}}(\lambda) = \frac{hc}{\lambda}$$

Here, h represents Planck's constant (6.626×10^{-34} J.s), and c represents the speed of light (2.998×10^{8} m/s). The energy of a number, N_{photons}, of moles of photons of a certain wavelength can described by including Avogadro's constant, N_{A}:

$$E_{\text{photons}}(\lambda) = \frac{N_{\text{photons}} N_{\text{A}} hc}{\lambda} \tag{1.3.3}$$

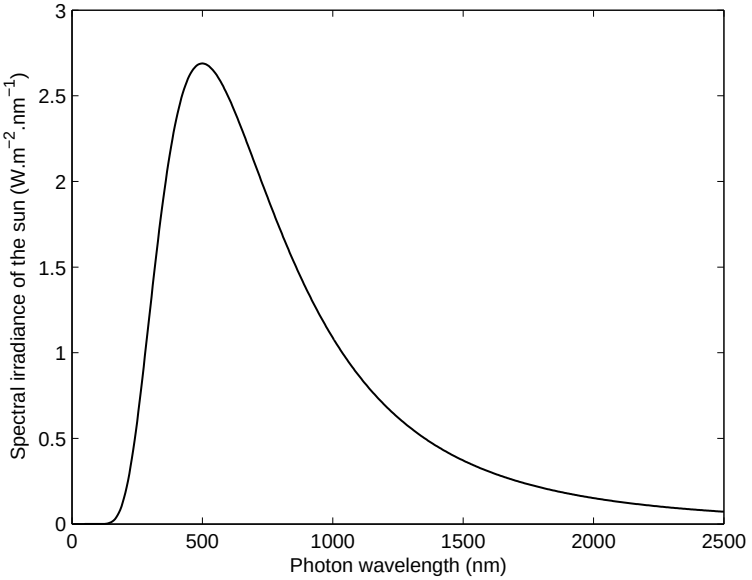


Figure 1.3.3: Spectral irradiance of the sun.

1.3.3.2 Spectral irradiance

The work of Planck (1901) extends to the development of a mathematical model to estimate the amount of energy provided by a black body over a spectrum of photon wavelength. This measure of energy can be defined as the spectral irradiance of the black body, which is the amount of energy per unit time per unit area per wavelength range produced by the body, shown often in the unit form of W/m^2.nm. The spectral irradiance is dependent on two variables: T, the blackbody temperature, and again, λ, photon wavelength. The equation for this correlation is given as:

$$I(T,\lambda) = \frac{2hc^2}{\lambda^5\left[e^{\frac{hc}{k\lambda T}} - 1\right]} \tag{1.3.4}$$

The only new constant introduced here is k, which is Boltzmann's constant (1.381×10^{-23} J/K). The usefulness of this relationship is evident in its application to the sun (for which, the blackbody surface temperature is approximately 5800 K), and thus how much energy it provides to the earth. At each photon wavelength, the equation reveals how much spectral irradiance or energy per unit area is provided to the earth; this is demonstrated in figure 1.3.3. The application of spectral irradiance to estimating biomass growth rates will be more closely examined in chapter 3.

1.3.3.3 Entropy

The issue of photon entropy and its application to a system analysis such as photosynthesis is one of contention. In the past, the conceptual model of a photon gas has been developed and taught (Leff, 2002). In this model, a group of photons is thought to occupy a particular volume of physical space, a cavity, at a certain pressure and temperature. As a result, the entropy of the photon becomes a function of this volume V and temperature T, with constant b:

$$\hat{S}_{\text{photon}}(V,T) = \frac{4}{3}bVT^3$$

Considering a fixed volume of a black body such as the sun with a known blackbody radiation temperature, this model appears effective. However, a number of concerns arise with the variables of volume and temperature in the application of this model to a natural process such as photosynthesis: what volume does a photon gas entering a photosynthetic organism occupy? What shape can one assume the particles to be? What can one consider the temperature of these photons to be?

Indeed, criticism of this model for the application of a photon absorption in a photosynthetic system by Kahn (1961) involves the discussion of the temperature at which the photon entropy is considered. The author states that the temperature of a single photon or group of photons is not easily definable, and that it cannot be simply considered to be that of the atmospheric surroundings, or that of the black body that the photons originate from. The model, it seems, is fallible to the application being considered here.

Therefore, the alternative perspective to examine now is the consideration of photons entering a photosynthetic system as a collection or group of individual photons, rather than a photon gas of a certain volume and temperature. Recent work by Kirwan (2004) suggests that photons carry an intrinsic or inherent entropy that is finite and constant, unlike a photon gas. The author maintains that this entropy does not vary according to wavelength, which affects particle size. Although the photons still occupy a region of physical space, their entropy is unaffected by volume. Kirwan (2004) derives this entropy to be:

$$\hat{S}_{\text{photon}} = \frac{4}{3}kA_T$$

Again, k is Boltzmann's constant (1.381×10^{-23}J/K). A_T is a dimensionless constant between 0.75, for a single photon, and 3, for a group or collection of photons. Since the analysis of the operation of photosynthesis involves the

absorption of groups of photons or quanta, the value of A_T can be fixed as 3, and thus the photon entropy definition reduces to:

$$\hat{S}_{\text{photon}} = 4k = 5.524 \times 10^{-23} \text{ J/K} \tag{1.3.5}$$

Finally, there remains one last perspective or viewpoint to consider regarding the photon entropy. Gudkov (1998) speculates that light from a blackbody radiation source is of such high-grade energy that it does not possess any inherent entropy. This would, in terms of photon entropy as a value, mean that:

$$\hat{S}_{\text{photon}} = 0 \text{ J/K} \tag{1.3.6}$$

To some extent, Lineweaver and Egan (2008) agree with this perspective, in that the light received by the earth contains high-grade energy. However, the authors contend that this light is both possessive of high-grade energy *and* low-entropy, as opposed to having no entropy at all. The authors also make the point that biological systems on earth would not be able to utilise this energy if it were high-entropy.

The question at hand is thus: can photon entropy be neglected for the basis of calculation if the light entering photosynthetic organisms is sufficiently low-entropy? Since quantifiable amounts for photon entropy are expressed for the perspective of Kirwan (2004) in equation 1.3.5, and for the viewpoint made mention of by Gudkov (1998) in equation 1.3.6, a comparison will be able to be drawn from these. Thus, the significance of the photon entropy term will be revealed, and the answer to this question indicated in the forthcoming analysis.

1.3.4 Quantum requirement

As mentioned in section 1.2, the main objective of this dissertation is to be able to model the photosynthesis reaction or process as a function of photon input. Thus, it is required to establish some form of basis from literature to enable comparisons to be made with the mathematical model that evolves from this analysis.

Equation 1.3.2 shows the uptake of six moles of carbon dioxide, and the subsequent production of six moles of oxygen, amongst the consumption of water and production of glucose. From photosynthesis research standards, the photon yield or quantum yield, commonly represented by the symbol ϕ_a, is defined as the number of moles of carbon dioxide consumed or moles of oxygen evolved per photon or quanta (Björkman and Demmig, 1987). The inverse of

this, the quantum requirement (QR), is thus the number of moles of photons or quanta required to allow the uptake of one mole of carbon dioxide or the production of one mole of oxygen:

$$\mathrm{QR}_{\mathrm{O}_2} = \frac{1}{\phi_a}$$

It follows mathematically from this that six times this number or value of $\mathrm{QR}_{\mathrm{O}_2}$ would be the number of photons required to synthesise one mole of glucose:

$$\mathrm{QR}_{\mathrm{glucose}} = 6 \times \mathrm{QR}_{\mathrm{O}_2}$$

Experimental literature approaches the finding of the value of the quantum requirement by determining and comparing the amount of photons absorbed by the photosynthesis system (plants or algae) with the amount of carbon dioxide reduced or the amount of oxygen released from the system (Zeinalov and Maslenkova, 1999).

Björkman and Demmig (1987) report that although many different species of plants and algae have been studied, the quantum requirement value in each study varies little. This can be explained by the reasoning that the photosynthetic pathway, or the general physiological mechanism in which photosynthesis occurs, in each organism is similar. Schmid and Gaffron (1967) confirm this by stating that differences in plant structure or chlorophyll content do not alter the quantum requirement. The result of this perspective is beneficial; the analysis being made in this dissertation is not limited to a specific species of plant or algae, but rather to the photosynthesis reaction in general.

During the mid-twentieth century, a difference in opinion on what the value of the quantum requirement should be emerged between two leading photosynthesis scientists, Warburg and Emerson. Warburg was of the opinion that the photosynthesis mechanism required 3 to 4 moles of photons for the evolution of one mole of oxygen, whereas Emerson believed that the quantum requirement was greater than this: in the region of 8 to 12 moles of photons (Govindjee, 1999).

In Warburg's last paper (Warburg et al., 1969), *Chlorophyll catalysis and Einstein's law of photochemical equivalence in photosynthesis*, Govindjee (1999) makes the point that Warburg had in fact produced a result similar to that of Emerson's quantum requirement for oxygen production. Emerson's perspective is now widely accepted as the correct one (Chain and Arnon, 1977), and thus that a photon requirement for photosynthetic organisms in the region of

8 to 12 moles of photons can be expected. Table 1.3.1 offers a fairly extensive list of quantum requirement values from different experimental and theoretical literature sources:

Author (Year)	QR for Oxygen Evolution (QR_{O_2})	QR for Glucose Synthesis ($QR_{glucose}$)
Andriesse and Hollestelle (2001)	10	60
Beadle and Long (1985)	8	48
Björkman and Demmig (1987)	$8.43 - 10.43$	$50.6 - 62.6$
Fragata and Viruvuru (2008)	$8 - 12.5$	$48 - 75$
Govindjee et al. (1968)	8	48
Govindjee (1999)	$8 - 12$	$48 - 72$
Ley and Mauzerall (1982)	$9 - 11$	$54 - 66$
Ley (1986)	$8.6 - 12.2$	$52 - 73$
Melis (2009)	9.5	57
Schmid and Gaffron (1967)	10	60
Warner and Berry (1987)	$6 - 8$	$36 - 48$
Average/Mean Value	10.3	61.7

Table 1.3.1: Comparative values of photosynthesis quantum requirements from literature.

The issue at stake now is to determine which values should be used for comparison with the analysis in this dissertation. In the forthcoming analysis, quantum requirements will be modelled per mole of glucose produced by the photosynthesis process. Since some of the tabulated values are expressed as a range of values, both a minimum and a maximum photon requirement are available for usage. From this, an average or mean value for the quantum requirement of glucose synthesis is calculated as 61.7 moles of photons per mole of glucose. In the forthcoming analysis the quantum requirement calculated theoretically can be compared to this mean value.

1.3.5 Photosynthetic efficiency and growth rates

In addition to the goal of determining a theoretical quantum requirement of photosynthesis, it is also an objective of this dissertation to further interest in theoretical capabilities of the process by examining photosynthetic growth rates. In chapter 3, theoretical growth rates will be calculated and compared with experimental growth rates from literature. An important concept to be utilised in this comparison is that of photosynthetic efficiency. Generally,

photosynthetic efficiency, η, may be defined as:

$$\eta = \frac{\text{Light energy used to produce biomass}}{\text{Total light energy received}}$$

In order to correlate the ratio of these energies, the concept of flux becomes a useful and necessary one. The quantity of total light energy received may be quantified by spectral irradiance, which is given in energy per square metre per second (energy flux). The energy used in the production of biomass (simplified in this analysis as glucose) will require two aspects. The first is the energy required to synthesise one mole of glucose; this is the quantum requirement, and the entire focus of chapter 2. The second aspect is a physical or mass measure of biomass that is grown per metre square per second, which is therefore a growth rate or mass flux.

Of interest, Andriesse and Hollestelle (2001) approach photosynthetic efficiency in a somewhat different manner. By drawing a correlation between the mass fluxes of incoming photons and the carbohydrate or glucose molecules formed during the process, and then relating it to the transport phenomena of a simplified glucose-water photosynthetic system, they are able to calculate photosynthetic efficiencies. In their analysis, the thermal conductivity, diffusion coefficient and atomic density are utilised to make this correlation, with considerable discussion on how variations in the diffusion coefficient affect the calculated efficiencies. In the work presented in this dissertation, though, focus will kept on combining the aspects of spectral irradiance, absorbance and quantum requirement as means of determining photosynthetic efficiencies and growth rates. The predicted and measured efficiencies by Andriesse and Hollestelle (2001) will prove as interesting material for comparison and discussion in chapter 3.

Comparable growth rates from literature will vary in the form that they are presented in. Moss (1967) reports that some crops will consume a maximum of approximately 6.0 $\mathrm{g/m^2}$.hr of carbon dioxide in direct sunlight. Doucha et al. (2005) indicates a maximum oxygen evolution rate of 7.1 $\mathrm{g/m^2}$.hr for the *Chlorella* species. From the exploration of light-dependent and light-independent processes of photosynthesis in sections 1.3.1.2 and 1.3.1.3, it has been implied that the rate of oxygen evolution and carbon dioxide are not simply stoichiometrically related according to equation 1.3.2. Andriesse and Hollestelle (2001) point to experimental results by Goudriaan and van Laar (1994) that between 11 μg and 14 μg of carbon dioxide are absorbed in plants

for every joule of incident light received. Thus, flux values for growth or energy in per square metre per second units are not available.

However, this does not mean that these data cannot be reconciled or assimilated into a comparable form, and chapter 3 will demonstrate this by utilising the concepts of spectral irradiance and absorbance, as well as discussion on the rates of carbon dioxide uptake and oxygen evolution.

Chapter 2

Calculating the Quantum Requirement

2.1 Method of Approach

As mentioned in the section 1.3.1.3, the photosynthesis process is a complex bioprocess, with numerous activities and reactions occurring within cells of the organism. The approach to be applied is thus a thermodynamic model by means of overall balances, thus paying little attention to the intricacies of the process. This approach has been termed as the "black-box" method by Patel et al. (2005). In it, the inputs and outputs of the process are investigated and remain the focus, but the inner workings (individual reactions and pathways) and specifics are not considered. Figure 2.1.1 shows a basic example of how this technique might be applied. By applying this approach to the photosynthesis

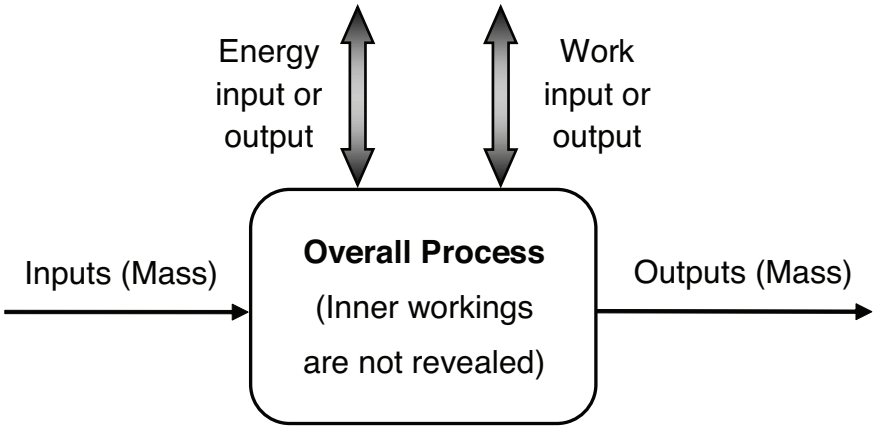


Figure 2.1.1: Diagram of the "black-box" approach, which considers the overall flows of mass, energy and entropy. The inner processes are not dealt with.

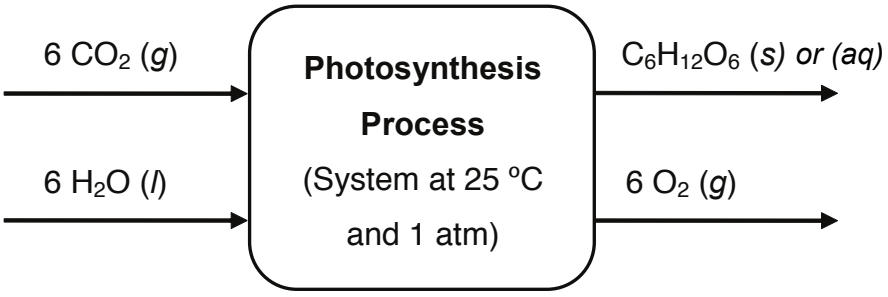


Figure 2.1.2: The mass balance for the photosynthesis process, with phases of the components indicated.

process, the mass, energy and entropy balances can be determined.

2.1.1 Mass and energy balances

The mass balance for the process is described in equation 1.3.2 and is illustrated in figure 2.1.2. An important consideration in the analysis of the photosynthesis process is the determination of the phases of the components. The energy, entropy and Gibbs free energy balances will all be affected, noticeably in some cases, from differences in thermodynamic properties between gas and liquid phases in particular.

The carbon dioxide absorbed is generally received from the atmosphere, or from an alternative gas mixture such as a flue gas, and therefore the carbon dioxide is in the gas phase. The water entering the photosynthetic system is, however, in the liquid phase, as this water is absorbed in such a state from soil by a root system in the case of many plants, and from a solution in the cases of hydroponic organisms such as algae.

With regard to the products, the phase of the sugar molecule glucose can be either solid or aqueous, as discussed previously in section 1.3.1.1, with the thermodynamic properties of enthalpy of formation and Gibbs free energy of formation being approximately the same in either phase. The oxygen evolved in the process is released to the atmosphere in the gaseous phase. Thus, the phases of the reactants and products have been determined; figure 2.1.2 demonstrates the phases and mass flows of these components. The temperature and pressure conditions of the photosynthesis process are ambient: 25 °C and 1 atm.

Traditionally, the energy balance for a system at constant pressure (in this

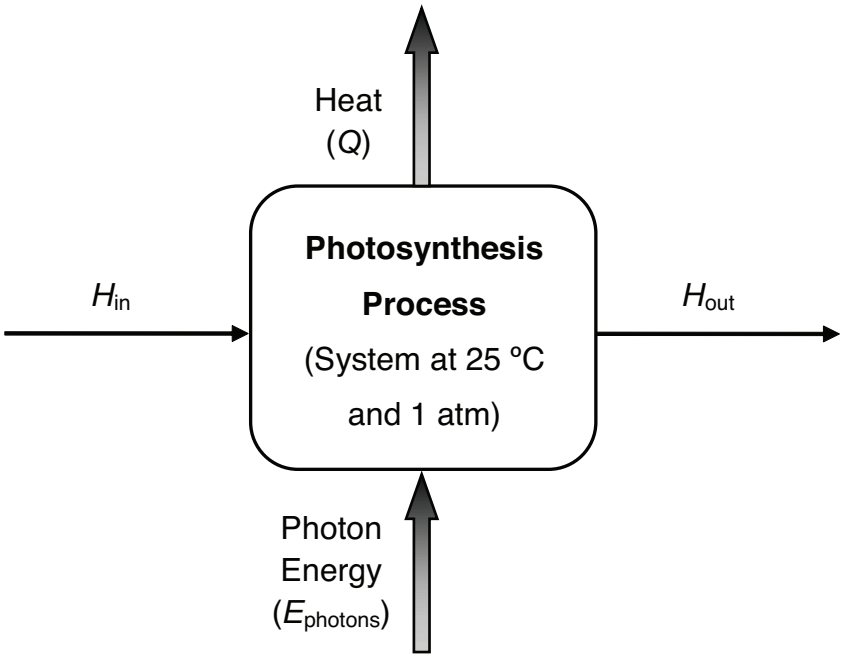


Figure 2.1.3: The energy balance for the photosynthesis process.

case constant atmospheric pressure) can be described as:

$$\Delta H_{\text{process}} + \frac{\Delta(u^2)}{2} + g\Delta z = Q + W_s$$

Since the photosynthetic organism is stationary, no changes in energy due to kinetic energy ($\frac{\Delta(u^2)}{2}$) or potential energy ($g\Delta z$) are applicable. There is also no addition or removal of shaft work (W_{s}) to the system, and this renders this term as zero. The energy balance thus far indicates that a change in enthalpy across the process will occur due to heat transfer. However, this heat transfer, as mentioned earlier in section 1.3.1.3, is the excess photon energy lost or rejected from the photosynthetic organism to the environment, since the photosynthetic reaction itself is endothermic.

The conventional energy balance does not, therefore, make account for a photon energy input term, and so this must be added to the energy balance in order to account for the energy installed by the photons into the photosynthetic system. The photon energy input term is a function of photon wavelength, as indicated in equation 1.3.3. The energy balance is now complete, as shown in figure 2.1.3, and can be mathematically represented as:

$$H_{\text{in}} + E_{\text{photons}}(\lambda) = H_{\text{out}} + Q$$

The enthalpy in (H_{in}) and enthalpy out (H_{out}) terms constitute the en-

thalpy owing to input and output of the reactants and products, respectively:

$$H_{\text{in}} = H_{\text{CO}_2} + H_{\text{H}_2\text{O}}$$

$$H_{\text{out}} = H_{\text{C}_6\text{H}_{12}\text{O}_6} + H_{\text{O}_2}$$

In order to determine a way of numerically representing the values of these components, a enthalpy basis must be established. Formation data for all the above substances is available at 25 °C and 1 atm, and considering these are the actual temperature and pressure conditions of the system, it seems convenient to set the basis as follows: the enthalpy of all elements at 25 °C and 1 atm is equal to zero. By the definition of the enthalpy of formation:

$$\Delta H^{\circ}_{\text{f,substance}} = H^{\circ}_{\text{substance}} - \sum \nu_i H^{\circ}_{\text{elements}}$$

Note that ν_i is the stoichiometric coefficient of an element i. Since the summation of the enthalpies of elements becomes a zero term, this renders the enthalpy of the compound equal to the enthalpy of formation of it:

$$H^{\circ}_{\text{substance}} = \Delta H^{\circ}_{\text{f,substance}} \tag{2.1.1}$$

Therefore, the enthalpies of the input and output streams of the photosynthetic system become:

$$H_{\text{in}} = 6\Delta H^{\circ}_{\text{f,CO}_2} + 6\Delta H^{\circ}_{\text{f,H}_2\text{O}}$$

$$H_{\text{out}} = \Delta H^{\circ}_{\text{f,C}_6\text{H}_{12}\text{O}_6} + 6\Delta H^{\circ}_{\text{f,O}_2}$$

The enthalpies of formation here are those for the phases of the components determined at the beginning of this section. The enthalpy change across the entire process is the difference between the input and output enthalpies:

$$\Delta H_{\text{process}} = \Delta H^{\circ}_{\text{f,C}_6\text{H}_{12}\text{O}_6} + 6\Delta \text{H}^{\circ}_{\text{f,O}_2} - 6\Delta \text{H}^{\circ}_{\text{f,CO}_2} - 6\Delta \text{H}^{\circ}_{\text{f,H}_2\text{O}}$$

The enthalpy change across the process thus resembles the enthalpy of reaction at ambient conditions (per mole of glucose produced), and a numerical value is obtained:

$$\Delta H_{\text{process}} = \Delta H^{\circ}_{\text{rxn}} = 2807.8\,\text{kJ/mol}$$

The photon energy can be expressed by Planck's expression, as demonstrated in section 1.3.3.1, and N_{photons} represents the number of moles of photons of a particular wavelength to equate the energy balance from equation 1.3.3:

$$E_{\text{photons}}(\lambda) = \frac{N_{\text{photons}} N_{\text{A}} hc}{\lambda} = \Delta H^{\circ}_{\text{rxn}} + Q$$

This can be rearranged as:

$$N_{\text{photons}} = \frac{\lambda}{N_{\text{A}} hc} \left(\Delta H^{\circ}_{\text{rxn}} + Q\right)$$

Therefore, a relationship between the number of photons, N_{photons}, and the wavelength, λ, has been established. However, the value of the heat rejected, Q, to the environment from the photosynthesis system is not known, and so the next step is to analyse the entropy balance of the process, in order to determine how this might affect the mathematical modelling developed thus far. As a final point, it should be important to note that number of photons, N_{photons}, required to satisfy the enthalpy of reaction for a mole of glucose, corresponds to the quantum requirement, $\text{QR}_{\text{glucose}}$, of glucose production:

$$\text{QR}_{\text{glucose}} = \frac{\lambda}{N_{\text{A}} hc} \left(\Delta H^{\circ}_{\text{rxn}} + Q\right) \tag{2.1.2}$$

2.1.2 Entropy balance

The entropy balance for the photosynthesis process is shown diagrammatically in Figure 2.1.4 and can be represented in an equation as:

$$S_{\text{in}} + S_{\text{gen}} + S_{\text{photons}} = S_{\text{out}} + \frac{Q}{T} \tag{2.1.3}$$

Several aspects of this balance require discussion and explanation. The entropy flow terms, S_{in} and S_{out}, correspond to the entropy flows of the reactants and products, respectively. The heat rejected, Q, to the surroundings from the system is done so at a particular temperature, T, and this is the temperature at which the process operates. In this case, temperature T is the ambient temperature, T_{o}.

S_{gen} is the internal entropy that is generated during the process and is a direct indication of irreversibility: higher values of S_{gen} will announce higher irreversibilities in the process. The entropy contained by the incoming photons

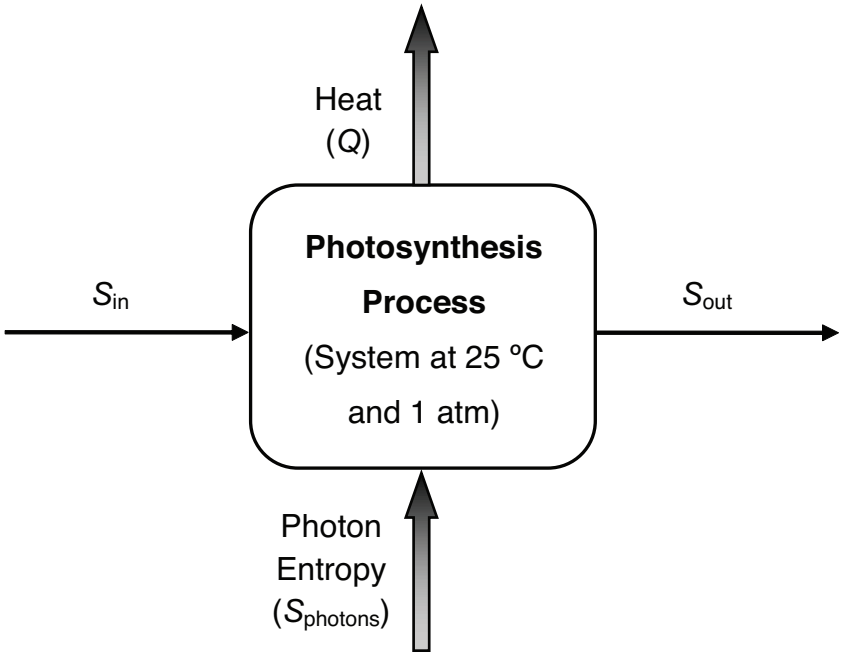


Figure 2.1.4: The entropy balance for the photosynthesis process.

is represented by the term S_{photons}, which can expanded to:

$$S_{\text{photons}} = N_{\text{photons}} N_{\text{A}} \hat{S}_{\text{photon}} \tag{2.1.4}$$

N_{photons} again represents the number of moles of photons required to equate the entropy balance. $\hat{S}_{\text{photon}}$ expresses the entropy of a single photon. Multiplying it with Avogadro's number, N_{A}, results in a value for the entropy of a mole of photons. The value of $\hat{S}_{\text{photon}}$ is an issue of debate, as demonstrated earlier in section 1.3.3.3. However, as mentioned, two scenarios and values of $\hat{S}_{\text{photon}}$ will be dealt with for comparative purposes.

Returning to equation 2.1.3, it is possible, as with the enthalpy balance, to expand the entropy in (S_{in}) and entropy out (S_{out}) terms to the sum of the entropy of the reactants and products, respectively:

$$S_{\text{in}} = S_{\text{CO}_2} + S_{\text{H}_2\text{O}}$$

$$S_{\text{out}} = S_{\text{C}_6\text{H}_{12}\text{O}_6} + S_{\text{O}_2}$$

By the definition of the entropy of formation, the equation can be rearranged so that the entropy of each substance is described as the sum of the entropy of formation and the sum of the entropy of each element of the sub-

stance:

$$S^{\circ}_{substance} = \Delta S^{\circ}_{\text{f,substance}} + \sum \nu_i S^{\circ}_{\text{elements}}$$

To eliminate the entropy of each element, an entropy basis is again set as: the entropy of all elements at 25 °C and 1 atm is equal to zero. With this basis and the definition of entropy of formation, the summation of the entropy of the elements becomes a zero term, and the entropy of the substance becomes equal to the entropy of formation of it. Therefore, the entropy terms of the input and output streams of the photosynthetic system become:

$$S_{\text{in}} = 6\Delta S^{\circ}_{\text{f,CO}_2} + 6\Delta S^{\circ}_{\text{f,H}_2\text{O}}$$

$$S_{\text{out}} = \Delta S^{\circ}_{\text{f,C}_6\text{H}_{12}\text{O}_6} + 6\Delta S^{\circ}_{\text{f,O}_2}$$

The entropy of formation of each substance here are those for the phases of the components determined at the beginning of this section, and formation data is available at 25 °C and 1 atm. The entropy change across the entire process is thus difference between the input and output enthalpies:

$$\Delta S_{\text{process}} = \Delta S^{\circ}_{\text{f,C}_6\text{H}_{12}\text{O}_6} + 6\Delta \text{S}^{\circ}_{\text{f,O}_2} - 6\Delta \text{S}^{\circ}_{\text{f,CO}_2} - 6\Delta \text{S}^{\circ}_{\text{f,H}_2\text{O}}$$

The entropy change across the process therefore resembles the entropy of reaction at ambient conditions (per mole of glucose produced), and a numerical value is obtained:

$$\Delta S_{\text{process}} = \Delta S^{\circ}_{\text{rxn}} = -0.252\,\text{kJ/mol}$$

Interestingly, this negative value is the negative entropy of the photosynthesis process or system, as confirmed by Yourgrau and van der Merwe (1968). In order to adhere to the Second Law of Thermodynamics, there must be a positive increase in the entropy of the surroundings (the region lying outside of the system) equal to or greater than the absolute value of the change in entropy of the system, so that overall entropy of the universe (combining the system and its surroundings) is equal to or greater than zero:

$$\because \Delta S_{\text{universe}} \geq 0$$

$$\because \Delta S_{\text{universe}} = \Delta S_{\text{system}} + \Delta S_{\text{surroundings}}$$

$$\because \Delta S_{\text{system}} < 0$$

$$\therefore \Delta S_{\text{surroundings}} > 0$$

$$\therefore \Delta S_{\text{surroundings}} \geq |\Delta S_{\text{system}}|$$

2.1.3 Gibbs free energy definitions

The implementation of Gibbs free energy data and definitions is important at this point, as it is capable of integrating and creating both energy and entropy balances towards a common goal: in this case, determining the number of moles of photons required to synthesise one mole of glucose. This ability of combining the two types of balances is apparent from the very definition of Gibbs free energy:

$$G = H - TS \tag{2.1.5}$$

Again, before proceeding any further, it is necessary to establish a basis for Gibbs free energy, as was done for the energy balance. The basis is set so that the Gibbs free energy of all elements at 25 °C and 1 atm is equal to zero. The input and output Gibbs free energies are:

$$G_{\text{in}} = G_{\text{CO}_2} + G_{\text{H}_2\text{O}}$$

$$G_{\text{out}} = G_{\text{C}_6\text{H}_{12}\text{O}_6} + G_{\text{O}_2}$$

With this basis now in position, the Gibbs free energy of each substance or compound reduces to its standard Gibbs free energy of formation for the relevant component phase. This follows the same basic method and result as with the enthalpy and entropy terms in sections 2.1.1 and 2.1.2. The overall change in Gibbs free energy is thus the difference between the reactants and products, with stoichiometric coefficients being applied:

$$\Delta G_{\text{process}} = \Delta G^{\circ}_{\text{f,C}_6\text{H}_{12}\text{O}_6} + 6\Delta \text{G}^{\circ}_{\text{f,O}_2} - 6\Delta \text{G}^{\circ}_{\text{f,CO}_2} - 6\Delta \text{G}^{\circ}_{\text{f,H}_2\text{O}}$$

The Gibbs free energy change across the process thus resembles the Gibbs free energy of reaction (per mole of glucose produced), and a numerical value is obtained:

$$\Delta G_{\text{process}} = \Delta G^{\circ}_{\text{rxn}} = 2883.0\,\text{kJ/mol}$$

Now that the Gibbs free energy of the process can be described quantitatively, the issue of combining the energy and entropy balances must be properly considered. The definition of Gibbs free energy, as shown in equation 2.1.5, can be applied to the substance inputs and outputs of the photosynthesis pro-

cess, and the difference between these terms is the change in Gibbs free energy across the process:

$$G_{\text{in}} = H_{\text{in}} - T_{\text{o}} S_{\text{in}}$$

$$G_{\text{out}} = H_{\text{out}} - T_{\text{o}} S_{\text{out}} \tag{2.1.6}$$

$$\Delta G_{\text{process}} = G_{\text{out}} - G_{\text{in}} \tag{2.1.7}$$

Returning to the energy and entropy balances developed so far, the following terms can be derived and rearranged from them:

$$H_{\text{in}} = H_{\text{out}} + Q - E_{\text{photons}}(\lambda)$$

$$S_{\text{in}} = S_{\text{out}} + \frac{Q}{T_{\text{o}}} - S_{\text{gen}} - S_{\text{photons}}$$

Substituting these two expressions in the definition of Gibbs free energy for the input stream obtains the following expression, which can then be simplified to:

$$G_{\text{in}} = H_{\text{out}} - E_{\text{photons}}(\lambda) - T_{\text{o}} \left(S_{\text{out}} - S_{\text{gen}} - S_{\text{photons}} \right) \tag{2.1.8}$$

The major step now is to substitute equations 2.1.8 and 2.1.6 into expression 2.1.7 so that resulting expression may be reduced to:

$$\Delta G_{\text{process}} = E_{\text{photons}}(\lambda) - T_{\text{o}} \left(S_{\text{gen}} + S_{\text{photons}} \right) \tag{2.1.9}$$

Further adjustment is applied by substituting the definition for energy of photons, $E_{\text{photons}}(\lambda)$, from equation 1.3.3, and the definition of the entropy of photons, S_{photons}, from equation 2.1.4:

$$\Delta G_{\text{process}} = \frac{N_{\text{photons}} N_{\text{A}} hc}{\lambda} - T_{\text{o}} \left(S_{\text{gen}} + N_{\text{photons}} N_{\text{A}} \hat{S}_{\text{photon}} \right)$$

In order to solve for the number of moles of photons, N_{photons} must be made the subject of the formula by rearranging the above expression:

$$N_{\text{photons}} = \frac{\Delta G_{\text{process}} + T_{\text{o}} S_{\text{gen}}}{N_{\text{A}} \left(\frac{hc}{\lambda} - T_{\text{o}} \hat{S}_{\text{photon}} \right)}$$

This is thus the main result of the method of analysis. Again, as explained in section 2.1.1 with equation 2.1.2, it should be important to note that the number of photons required to satisfy the Gibbs free energy of reaction for a mole of glucose, N_{photons}, corresponds to the quantum requirement of glucose

production, $\mathrm{QR}_{\mathrm{glucose}}$:

$$\mathrm{QR}_{\mathrm{glucose}} = \frac{\Delta G^{\circ}_{\mathrm{rxn}} + T_{\mathrm{o}} S_{\mathrm{gen}}}{N_{\mathrm{A}} \left(\frac{hc}{\lambda} - T_{\mathrm{o}} \hat{S}_{\mathrm{photon}} \right)} \tag{2.1.10}$$

How the derived quantum requirement values compare with quantum requirement values from literature remains to be seen in the following results section.

2.2 Results of the Analysis

2.2.1 Zero heat scenario

In examining the theoretical quantum requirement of the photosynthesis process, attention must first be drawn to the relationship established from the energy balance, as shown in equation 2.1.2 and derived in section 2.1.1. Here, as suggested by the nature of the balance, entropy is not being considered, and the focus is more on the correlation between quantum requirement, $\mathrm{QR}_{\mathrm{glucose}}$, and Q, the heat transferred by the photosynthetic system to or from the surroundings. A primary limit of operation, and indeed a minimum one, of the photosynthesis system is formed in the scenario where no energy transfer between the system and surroundings occurs, thus rendering the value of Q equal to zero. This reduces equation 2.1.2 to:

$$\mathrm{QR}_{\mathrm{glucose}} = \frac{\lambda}{N_{\mathrm{A}} hc} \left[\Delta H^{\circ}_{\mathrm{rxn}} \right]$$

In figure 2.2.1, the quantum requirement according to this equation in the spectrum of photosynthetically active radiation (400 nm to 700 nm) is shown. The gradient of the curve is linear, and the quantum requirement value increases with wavelength. At 400 nm, 9.39 moles of photons are required for the photosynthesis of one mole of glucose, and at 700 nm, 16.4 moles of photons are required. The average quantum requirement value calculated from literature of 61.7 moles of photons is represented as a horizontal line, unvarying with photon wavelength.

The theoretical quantum requirement values predicted by the above equation are much less, regardless of photon wavelength, than the average quantum requirement from literature. By the very nature of the equation 2.1.2, any further moles of photons of a certain wavelength added to the system will increase the heat rejected to the surroundings by the system. As said, this scenario of

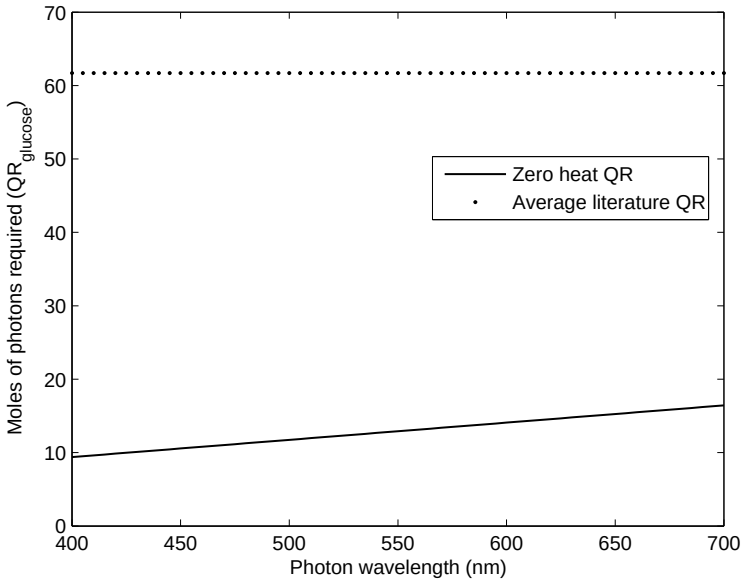


Figure 2.2.1: Minimum quantum requirement for glucose synthesis from energy balance corresponding with the scenario of zero heat (Q = 0), compared to the average value quoted by literature.

zero heat rejected to the surroundings thus forms a minimum limit of operation of the photosynthetic system; this is an absolute minimum number of moles of photons, according to the energy balance, that can added to the system in order to synthesise one mole of glucose.

2.2.2 Reversible, zero photon entropy scenario

With the quantum requirement from the energy balance derivation considered, the more advanced approach of incorporating the concept of entropy and Gibbs free energy, as shown in sections 2.1.2 and 2.1.3 and finalised in equation 2.1.10, can be examined. A limit of operation can be ascertained by applying two limiting conditions. The first of these is that the photosynthesis system is assumed to be perfectly reversible, with the term $S_{\text{gen}} = 0$. The second of these is the suggested viewpoint of Gudkov (1998) in equation 1.3.6 that photon entropy is zero ($\hat{S}_{\text{photon}} = 0$ J/K). Equation 2.1.10 simplifies to the following with these conditions in place:

$$\text{QR}_{\text{glucose}} = \frac{\Delta G^{\circ}_{\text{rxn}}}{N_{\text{A}} \left(\frac{hc}{\lambda}\right)} \tag{2.2.1}$$

Figure 2.2.2 demonstrates the quantum requirement according to this sim-

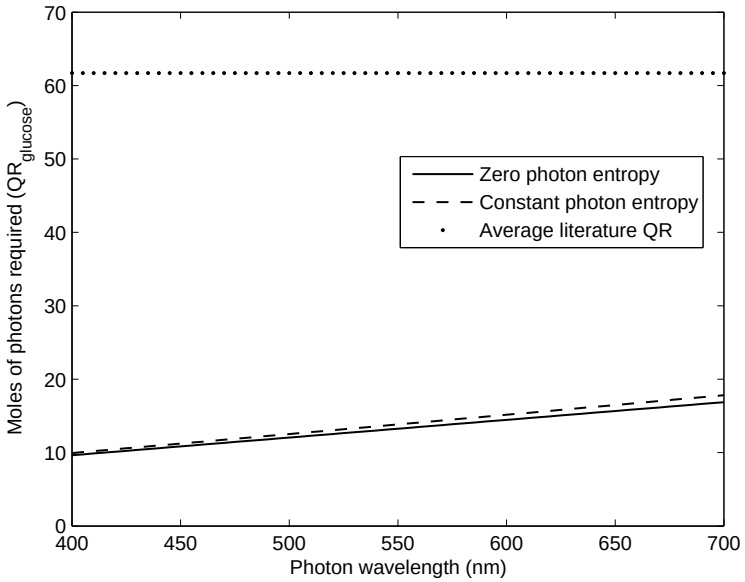


Figure 2.2.2: Minimum quantum requirement for reversible glucose synthesis with zero (Gudkov, 1998) and finite (Kirwan, 2004) values of photon entropy, compared to the average quantum requirement from literature.

plified equation, as well as for the scenario in the forthcoming subsection. The shape of this curve is again linear, with the quantum requirement increasing proportionally with photon wavelength.

As can be seen, the theoretical number of moles of photons required are far less than the average number predicted by literature. At the 400 nm mark, the theoretical number of photons required is 9.64, and at the 700 nm, the theoretical quantum requirement is 16.9 moles of photons. Again, this scenario forms a limit of operation with regard to internal entropy generated; this is absolute minimum number of photons required by the photosynthetic system, by way of the entropy balance, for it to produce one mole of glucose in a reversible manner.

2.2.3 Reversible, finite photon entropy scenario

In this section, the scenario where photon entropy is not zero, but rather finite, is examined. The constant value of photon entropy $\hat{S}_{\text{photon}} = 5.524 \times 10^{-23}\,\text{J/K}$, as given by Kirwan (2004) from equation 1.3.5 is applied to equation 2.1.10. The resultant curve of quantum requirement is no longer linear, and possesses a positively increasing gradient owing to addition of the constant $T_{\text{o}}\hat{S}_{\text{photon}}$

term:

$$\mathrm{QR}_{\mathrm{glucose}} = \frac{\Delta G^{\circ}_{\mathrm{rxn}}}{N_{\mathrm{A}}\left[\frac{hc}{\lambda} - (1.508 \times 10^{-20}\ \mathrm{J})\right]} \tag{2.2.2}$$

For comparative purposes, figure 2.2.2 displays both the zero entropy and finite photon entropy curves, along with the average quantum requirement suggested by literature. At any point along the PAR spectrum, the gradient of the finite photon entropy curve is greater than the curve developed with zero photon entropy.

It can be seen too that the number of moles of photons required for glucose synthesis, where photon entropy is finite, is slightly greater than the number of moles of photons required where photon entropy is considered to be zero. At 400 nm, 9.94 moles of photons are required for the photosynthesis of one mole of glucose, as opposed to 9.64 moles in the case of zero photon entropy. At 700 nm 17.8 moles are required, as opposed to 16.9 moles in the case of zero photon entropy. These amounts reiterate the non-linearity of the finite entropy curve.

Regardless of these small increases in quantum requirement from the zero photon entropy curve to the finite photon entropy curve, the number of moles of photons required for the finite entropy calculation is still far below the constant value averaged from literature. The effect made by including a finite photon entropy, as opposed to neglecting it and considering it to be zero, is thus a small one, as can be seen.

2.2.4 Increasing irreversibility

Since it has been established that photon entropy makes a slight difference to quantum requirement, the next step is to examine the effect of irreversibility on the quantum requirement. Thermodynamically, a value of $S_{\mathrm{gen}} = 0$ for the internal entropy generated by the process is an indication that the process is completely reversible. However, with values of $S_{\mathrm{gen}} > 0$, the process becomes irreversible. Thus, the consequence of an increasingly irreversible photosynthesis process on the quantum requirement can be evaluated by adjusting this term. Increasing values (from zero) of the internal entropy generated in the photosynthesis system, S_{gen}, are implemented. The scenario of finite photon entropy is utilised, and the two non-zero values of S_{gen} are shown in figure 2.2.3, alongside the average literature quantum requirement.

By observation, it can deduced that a larger irreversibility in the process increases the number of moles of photons required to satisfy the reaction. In

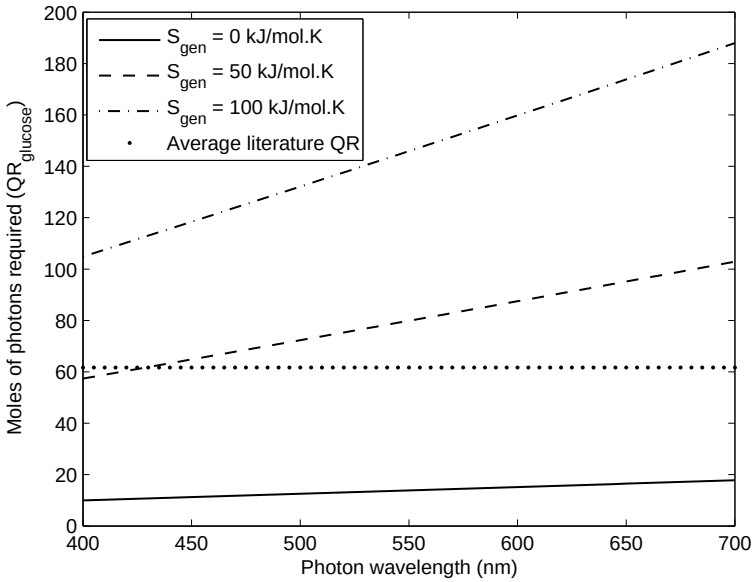


Figure 2.2.3: Minimum quantum requirement values for different and increasing values of internal entropy generated per mole of reaction (S_{gen}) of the process, in comparison with the average quantum requirement from literature.

figure 2.2.3, it is possible to interpolate between quantum requirement lines to estimate certain irreversibilities of the system. Depending on the wavelength of the photons, as well as the irreversibility term, it is possible for the theoretical quantum requirement to coincide with the average quantum requirement from literature.

For example, at a chlorophyll *a* absorbance peak of 680 nm an internally-generated entropy term of just greater than 26.3 kJ/mol.K would have a quantum requirement roughly on par with that of literature. For the limits of the photosynthetically active radiation spectrum (PAR), the value of S_{gen} would need to be 54.5 kJ/mol.K at 400 nm, and 25.8 kJ/mol.K at 700 nm, in order to equate the theoretical quantum requirement with that of the literature average.

Considering that the entropy change across the process or reaction is $\Delta S^{\circ}_{\text{rxn}} = -0.252\,\text{kJ/mol.K}$, the above amounts indicate that the process would have to be greatly irreversible in order to agree with literature average quantum requirement.

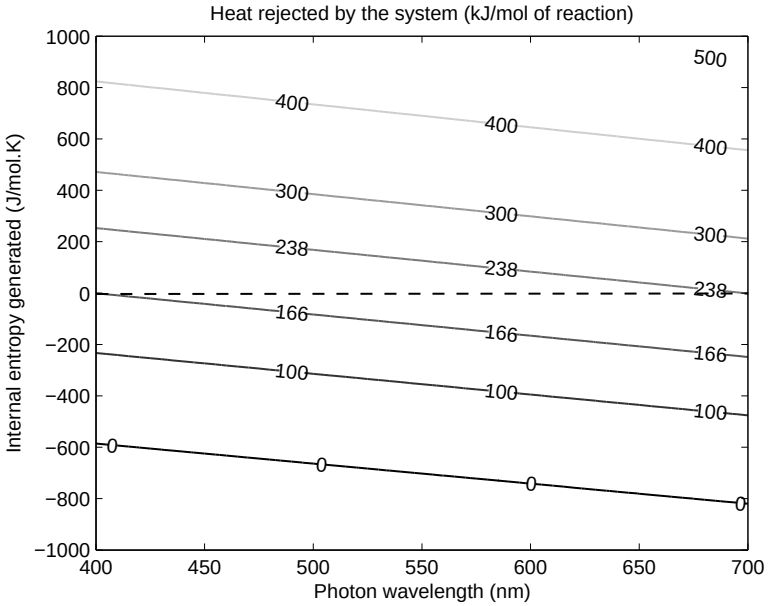


Figure 2.2.4: Contour plot of the heat rejected by the system (Q) as a function of internal entropy generated per mole of reaction (S_{gen}) for the finite photon entropy scenario. The dashed line indicates the process at reversible conditions, where $S_{\text{gen}} = 0$. Process irreversibility increases as one moves above this line. The contours for heat rejection at reversible conditions for photons of 400 nm and 700 nm occur and are shown with 166kJ/mol and 238kJ/mol, respectively.

2.2.5 Heat rejection and irreversibility

To further understand and ascertain what the limit of operation of the photosynthesis process is, the link between irreversibility and heat rejection must be examined according to the model that has been developed. It is possible to express the heat rejected by the system as a function of the internal entropy generated by the system, which is an indication of how reversible or irreversible the process is. A derivation of the following equation is not necessary here, but is included in appendix A for interest:

$$Q = TS_{\text{gen}} + T\hat{S}_{\text{photon}} \left[\frac{\Delta G_{\text{process}} + T_{\text{o}} S_{\text{gen}}}{\left(\frac{hc}{\lambda} - T_{\text{o}} \hat{S}_{\text{photon}} \right)} \right] + \Delta G_{\text{process}} - \Delta H_{\text{process}} \quad (2.2.3)$$

As before, the results of applying the two scenarios of zero entropy and finite, constant photon entropy must be compared. Figure 2.2.4 shows a contour graph of the situation of finite photon entropy. The necessity of using a contour plot is put forth by the heat rejected, Q, being dependent on two variables, S_{gen} and λ. The difference between $\Delta G_{\text{process}}$ and $\Delta H_{\text{process}}$ is a

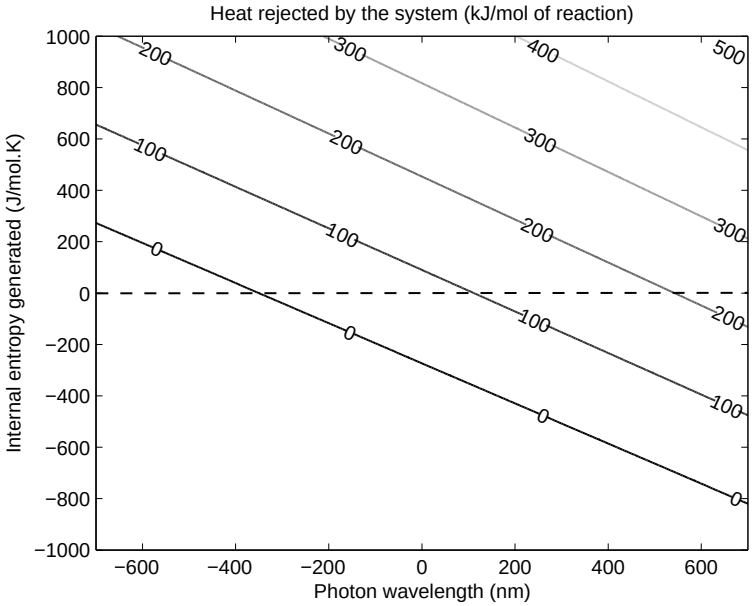


Figure 2.2.5: Contour plot of the heat rejected by the system (Q) as a function of internal entropy generated per mole of reaction (S_{gen}) for the finite photon entropy scenario. The graph is an extended version of figure 2.2.4, showing now the theoretical negative spectrum of photon wavelength. The dashed line indicates the process at reversible conditions, where $S_{\text{gen}} = 0$. Process irreversibility increases as one moves above this line. The intersection of contour $Q = 0$ with $S_{\text{gen}} = 0$ can be seen at a wavelength of -307 nm.

constant value, and the heat rejected, Q, is therefore only sensitive to changes in the two aforementioned variables, S_{gen} and λ.

The thermodynamically feasible region of operation is represented generally when $S_{\text{gen}} \geq 0$. When $S_{\text{gen}} = 0$, the process is perfectly reversible, but any positive values for this variable will indicate irreversibility in the process. It follows that the internal entropy generated by the process cannot be a negative number. Increasing irreversibility and thus the value of S_{gen} produces a relationship of increased heat rejection. The minimum heat rejected occurs therefore when the process is perfectly reversible. This amount varies between 166 kJ/mol of reaction at 400 nm, and 238 kJ/mol of reaction at 700 nm.

An interesting occurrence is observed when one attempts to set the process as both perfectly reversible ($S_{\text{gen}} = 0$) and adiabatic ($Q = 0$). Figure 2.2.5 is an extended version of figure 2.2.4, showing the theoretical negative spectrum of photon wavelength. An intersection of these curves is available at -307 nm, satisfying these conditions.

If equation 2.2.3 is examined, the difference between $\Delta G_{\text{process}}$ and $\Delta H_{\text{process}}$ will always be positive, as it has been set by the photosynthetic equation 1.3.2.

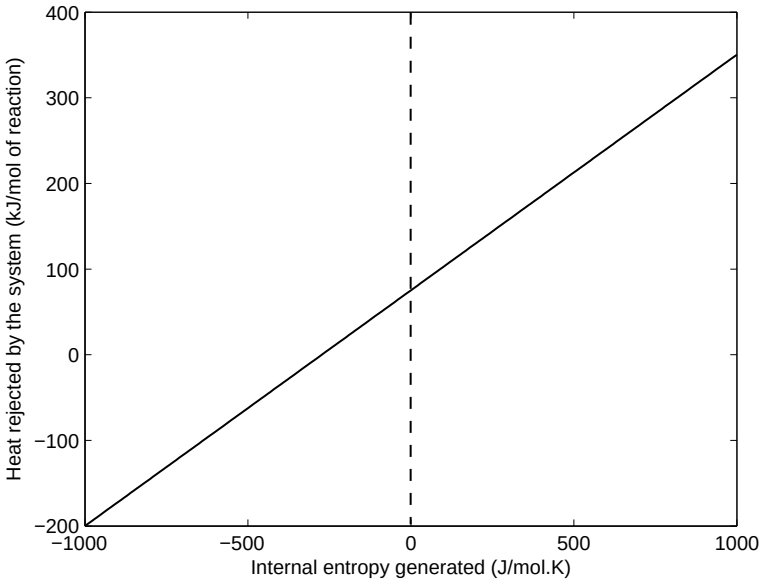


Figure 2.2.6: Heat rejected by the system (Q) as a function of internal entropy generated per mole of reaction (S_{gen}) for the zero photon entropy scenario. The dashed line indicates the process at reversible conditions, where $S_{\text{gen}} = 0$. Process irreversibility increases as one moves right of this line.

If S_{gen} and Q are set as zero, then the only remaining term, must be negative in order to satisfy the equation. The only way to do this is to set the photon wavelength. In reality, it is not possible to have photons of negative wavelength. The significance of this observation is that it is therefore not physically possible for the photosynthesis process to be both reversible and adiabatic. In addition to this point, it can be concluded that the process *must* reject heat, regardless of the degree of reversibility.

Attention is now turned to the situation where photon entropy is assumed to be zero. Equation 2.2.3 is greatly simplified to:

$$Q = TS_{\text{gen}} + \Delta G_{\text{process}} - \Delta H_{\text{process}}$$

Again, the difference between $\Delta G_{\text{process}}$ and $\Delta H_{\text{process}}$ is a constant value, and the heat rejected, Q, is now only dependent on and sensitive to changes of one variable, which is the internal entropy generated within the process, S_{gen}. The heat rejected, Q, is now independent of photon wavelength, λ, in this scenario. The linear relationship between Q and S_{gen} is indicated by figure 2.2.6. Again, the feasible region of operation for the photosynthesis process occurs when $S_{\text{gen}} \geq 0$. In this case, the minimum heat that can be rejected is 75.2kJ/mol of reaction, or glucose produced, when the process is considered to

be reversible. Thus, as observed before, the process must reject heat, whether it is reversible or irreversible.

2.3 Discussion and Conclusions

2.3.1 Photon entropy

Several points from the section of results require discussion. The first point of discussion is the issue of the intrinsic photon entropy and whether to include it or neglect it in the entropy balance. The results above have shown that the differences in quantum requirement for the scenario of zero photon entropy and for the scenario of finite, constant photon entropy are minor. Relative deviations can help to quantify these differences: at 400 nm, the quantum requirement where photon entropy is finite is 3.1% greater than that where photon entropy is considered zero. At 700 nm, this difference is 5.3%, with reference to the same relationship.

The effect of including photon entropy in calculations, therefore, is a small and fairly insignificant one. The perspective of Lineweaver and Egan (2008) that light is high-energy and low-entropy can be recalled and in some way confirmed in this regard; the energy of the photons influences the quantum requirement far more than the entropy of the photons.

For the purposes of simple estimations, it seems acceptable to neglect a finite value of photon entropy, approximating photon entropy as zero for simplicity. However, with that said, the truth and value of inherent photon entropy remains obscure; the viewpoint of zero photon entropy is not necessarily confirmed. In fact, literature seems to side more with the inclusion of a finite value for photon entropy. With the simplified and constant value proposed by Kirwan (2004), including it in calculations is the recommended course of action here.

2.3.2 Limits of operation

The second topic of discussion involves which limit of operation is to be selected as the correct one for the theoretical model developed. To begin with, the value of the limit of operation must be illustrated. The limit of operation is a boundary, in this case a minimum boundary, which indicates what the absolute minimum quantum requirement is in order to complete the photosynthesis reaction. Once this has been established, other aspects of the process, such

as the maximum biomass yield over a period of time, can be estimated. In essence, the limit of operation of this analysis is the theoretical best or greatest efficiency that the process can achieve.

The results displayed in this section put forward two prime candidates for the limit of operation: the scenario involving zero heat, and the scenario of a reversible process. In comparing the quantum requirement values of the two situations, the scenario of zero heat transfer evokes the smallest number for the quantum requirement, by use of the energy balance. However, if the internal entropy generated, S_{gen}, for this scenario is calculated, it is revealed to be a negative number. It is also a consistently negative number, regardless of whether photon entropy is zero or finite, and regardless of photon wavelength. This outcome is demonstrated in figures 2.2.4 and 2.2.6.

This is not a thermodynamically correct possibility. The overall change in entropy of the system is allowed to be negative, provided that entropy of the surroundings is increased. However, the actual internal entropy generated of a system must be zero, indicating a reversible system, or positive, indicating an irreversible system. This eliminates the possibility of the zero heat situation being the limit of operation. The correct limit of operation is thus the reversible system, in which heat must be rejected from the photosynthetic system to the surroundings. This limit of operation is applied in conjunction with the above decision to include a constant, finite value for photon entropy.

For approximate purposes, the correct limit of operation could also be the simpler case where photon entropy is neglected and assumed to be zero. Until there is a common consensus on the value and nature of photon entropy, the exact limit of operation is unknown. However, with that said, what is known is that the most defining aspect for the minimum quantum requirement or limit of operation of the photosynthesis process is the system state of being completely reversible.

The final point of discussion regards the actual differences between the theoretical and literature quantum requirement values. By demonstration of the thermodynamic analysis, the average literature quantum requirement is several times larger than the quantum requirements predicted in the zero heat and reversible scenarios. It would be daring to suggest that an entire collection of experimental literature is incorrect. Although, it is perplexing that several literature sources (Andriesse and Hollestelle, 2001; Beadle and Long, 1985; Schmid and Gaffron, 1967) do not seem to account for fluctuating photon energy due to the effect of wavelength, by only providing a single, constant

quantum requirement.

If the quantum requirements from literature are indeed considered to be correct, then the thermodynamic model has effectively indicated that the photosynthesis process in nature is a rather irreversible one, and does not utilise photon energy effectively. One might argue that because of these differences between theory and literature, opportunity exists in optimising the photosynthetic process. In terms of improving its efficiency of utilising solar energy, the advent of artificial photosynthesis (Listorti et al., 2009; Kalyanasundaram and Graetzel, 2010) may offer opportunities for this work. The hope here is that with improved efficiency, larger amounts of biomass can be grown artificially in comparison to amounts grown naturally, and thus accommodate the requirements of the biofuels and various other industries.

2.4 Further Analysis: Heat Rejection Feasibility

2.4.1 Macroscopic heat rejection

A purpose of this work is to determine if the quantum requirement averaged from literature is realistic, and what the implications of this are. According to the mathematical model developed, there are large discrepancies between the calculated quantum requirement for a reversible process and the average literature quantum requirement. In turn, the quantum requirement for the former (average from literature) will promote the rejection of different and increased quantities of heat in comparison to the former (reversible process).

Comparing this heat rejection in terms of feasibility can assist in determining whether or not the quantum requirement values seem reasonable. Ultimately, if the quantum requirement from literature produces amounts of heat that are too large to reject, the value of the quantum requirement is put into question.

Focus now shifts to the energy transfer from the photosynthesis system to the surroundings, or the heat rejected to the surroundings. Returning to and rearranging equation 2.1.2 to ensure heat, Q, is made the subject of the formula:

$$Q = \mathrm{QR}_{\mathrm{glucose}} \left(\frac{N_{\mathrm{A}} hc}{\lambda} \right) - \Delta H^{\circ}_{\mathrm{rxn}}$$

The model is now employed to utilise quantum requirement data from literature (recall the average literature quantum requirement of 61.7 moles of photons), in order to calculate the heat rejected by the system. This tech-

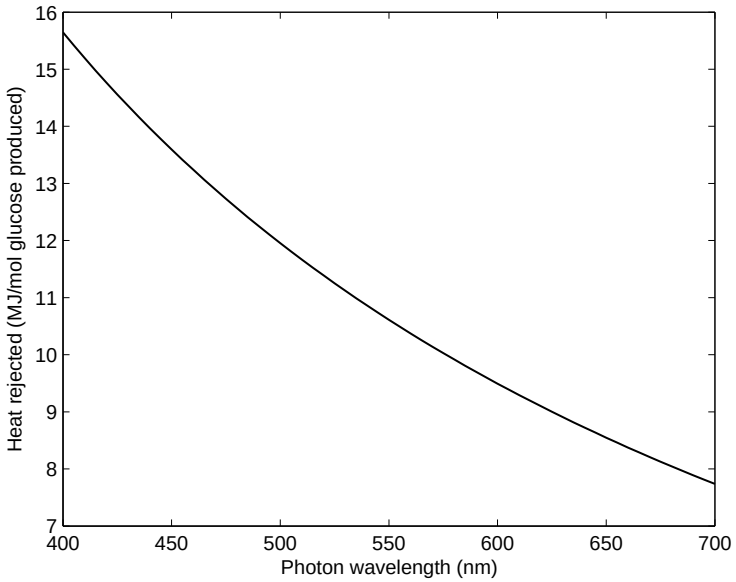


Figure 2.4.1: Heat rejected by the photosynthesis system utilising the average literature quantum requirement of 61.7 moles of photons at different wavelengths in the photosynthetically active radiation spectrum (PAR).

nique is applied in order to determine whether or not the amounts of energy rejected as heat could be considered as feasible, and thus if by this aspect the average quantum requirement from literature seems feasible. Figure 2.4.1 illustrates the non-linear curve resulting from this calculation. The set, unvarying quantum requirement value from literature produces different energy amounts that would be rejected as heat, depending on the wavelength of the incoming photons.

It can seen that these values for the heat rejected are large quantities, ranging from 15.6 MJ/mol at 400 nm, down to 7.7 MJ/mol at 700 nm, all per mole of reaction or mole of glucose produced. For comparison, in the case of utilising the quantum requirement for the reversible, finite-entropy scenario, these heat amounts from figure 2.2.4 are much less: 166 kJ/mol of reaction, at 400 nm, and 238 kJ/mol of reaction, at 700 nm.

As can be seen, the amounts of heat rejected by the irreversible process where average literature quantum requirement is utilised are far greater than those for the reversible case. However, while the former energy values are considerably bigger, they cannot provide sufficient insight on their own as to whether or not they can be rejected feasibly over a period of time. The same can be said of the heat amounts for the process using the reversible quantum requirement. Thus, a model of the rate of heat rejection, or heat rejection per

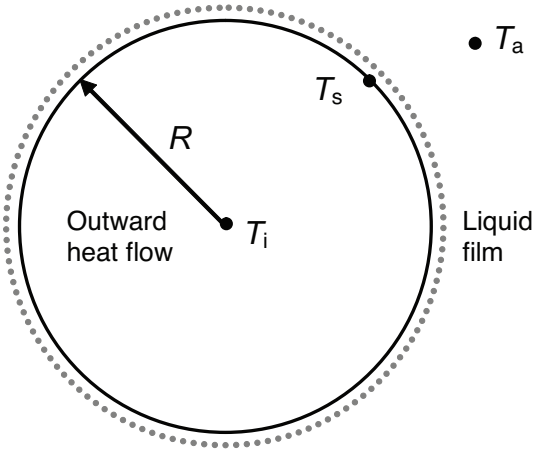


Figure 2.4.2: Heat transfer over a simplified, spherical algal cell. Heat transfer occurs in the direction outwards from the centre of the cell, as well as over the surface of the cell to the bulk fluid (water) over a film of the fluid.

time, is required in order to further investigate this query.

2.4.2 Microscopic model of heat rejection per time

Applying Fourier's law with a simple, steady-state heat transfer model for a plant or algae allows for the observation of internal temperature gradients. In all cases, the plant or algae is rejecting heat to its surroundings, implying that internal temperature of the organism must be higher than the ambient temperature for a gradient to exist. However, if this internal temperature is too high, the issue of heat damage to the cell becomes significant and of concern.

One of the greatest obstacles in the way of developing such a model lies in the difficulty of incorporating different plant geometries and inconsistent structural elements. With that said, some microalgae species seem approachable for heat transfer modelling for several reasons. Firstly, a major species of microalgae such *Chlorella* consists as a collection of consistently spherical cells surrounded by a bulk water medium in which they grow, say at an ambient water temperature of 25 °C (Graham and Wilcox, 2000). In addition to their mathematically simple area and volume, such a species is unicellular, meaning that one cell is an accurate representation of all the cells in the system.

Appendix B provides a full, comprehensive method detailing the derivation of the heat transfer model for a spherical microalgae species. It will not be included here due to its length, but should be perused for complete understanding. The basic functioning and capability of it can, however, be explained in brief, and the results of it can be shown.

It is necessary before continuing here, to differentiate between specific forms of heat loss or rejection. Q is defined in this work is the heat rejected to the surroundings per mole of reaction of glucose or biomass formed, and thus has units of kJ/mol. In the case now of establishing a heat transfer model, the rate of heat transfer or energy rejected per time will be applied as symbol q and having units of W.

Over a period of time, one mole of algae, approximated as glucose and therefore having a mass of 180.16 g, will be grown with a total heat rejection rate of q_{total}. In order to determine what the rate of heat rejection across one cell (q_{cell}) in that mass of algae is, the number of cells must be calculated. This can be achieved by establishing a representative radius for these cells, and hence the volume of each cell, and then approximating the density of the algae as a weighted average of glucose and water (1270 kg/m^3):

$$N_{\text{cells}} = \frac{180.16\ \text{g}}{\rho_{\text{average}} \left(\frac{4}{3}\pi R^3\right)}$$

With this knowledge, the total rate of heat rejection can be divided by the number of cells to determine the rate of heat rejection per cell:

$$q_{\text{cell}} = \frac{q_{\text{total}}}{N_{\text{cells}}}$$

Now, knowing what the rate of heat rejection per cell is, the model can begin to be developed. The assumption of steady state heat transfer is made in order to simplify the model. In essence, it can describe the temperature profile across the cell as the algae grows and as heat from the excess incoming photons is rejected from the cell to the surrounding water – figure 2.4.2 provides a graphic representation of this mechanism.

The model is able to predict the inner core temperature of a spherical cell as a function of its radius; the centre point of the cell is assumed to be the hottest location in order to promote outward heat flow. To re-iterate, the primary aim is to observe how the inner core temperature differs from the ambient, bulk water temperature. If the cell is operating well above the ambient temperature, then this is an indication that the cell would be likely to be damaged and not able to reject heat at such a rate.

In order to describe the rate of heat released by the cell at any point in the spherical cell, a generation term, α, must be introduced. α represents the amount of energy per time generated per volume of the sphere (W/m^3). It is defined such that the rate of heat generated at the surface, where the sphere

has a full radius of R, is equal to the rate of heat released by the cell:

$$\alpha = \frac{q_{\text{cell}}}{\frac{4}{3}\pi R^3}$$

By applying Fourier's law to determine the temperature differences over the cell, as well as over the film of water surrounding the cell, a number of combinable equations are formed. Again, Appendix B should be consulted for the derivation of these equations. The final equation is able describe the temperature difference between the inner core of the cell and the surrounding bulk water as a function of the cell radius, R, the heat generation term, α, the thermal conductivity of the cell material, k_{cell}, and the film transfer coefficient, h_{water}:

$$T_{\text{i}} - T_{\text{a}} = \frac{\alpha R}{3}\left(\frac{R}{2k_{\text{cell}}} + \frac{1}{h_{\text{water}}}\right)$$

2.4.3 Results and discussion

Comparison between the heats rejected for the reversible case and the irreversible case are made; the latter utilises the average literature quantum requirement, while the former utilises the quantum requirement for the reversible, finite-entropy scenario. A set wavelength of 680 nm for the incoming photons is used, as this is a common absorbance peak for chlorophyll *a* (Berg et al., 2002). For the reversible process, the heat rejected is 233 kJ/mol of glucose produced from figure 2.2.4, and for the irreversible process this heat rejected is 8.05 MJ/mol of glucose produced, from figure 2.4.1.

To demonstrate the numerical value of α, consider the aforementioned heat rejection per mole of glucose produced for the reversible and irreversible processes using photons of wavelength 680 nm. Choosing a particle or radius size for a cell, it is possible to determine the number of cells, N_{cells}, and thus the rate of heat rejection per cell, q_{cell}. Therefore, for a cell of 6 microns in radius, α will have a value of $1.65 \times 10^9\,\text{W/m}^3$ and $5.67 \times 10^{10}\,\text{W/m}^3$ for the reversible and irreversible processes, respectively.

The results of this model are shown in figure 2.4.3 and indicate that internal temperature of an algae cell will be much higher for the irreversible case where more heat is rejected per time. This is to be expected, as the total heat rejection for the average literature quantum requirement is much greater than for the reversible quantum requirement. The results also reveal that larger radii for spherical algae cells would possess higher inner core temperatures to allow such rates of heat rejection per cell. This can be explained since larger

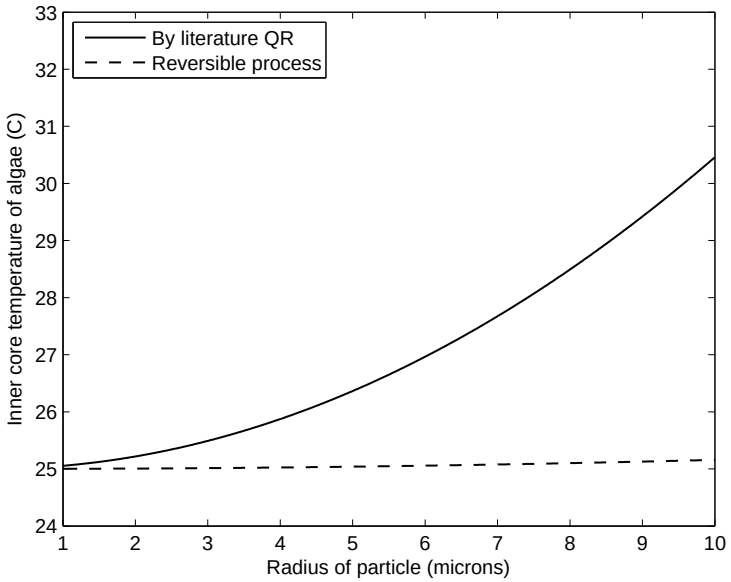


Figure 2.4.3: Inner core temperature of a microalgal cell with increasing radius size resulting from heat rejection. The ambient temperature is chosen to be 25 °C. Typical algae cells will range with radii between 1 and 6 microns (Graham and Wilcox, 2000). The heat rejected is compared for case of the average literature quantum requirement (the irreversible process) and for the quantum requirement from the reversible process. The incoming photons to the organism are of wavelength 680 nm, a common absorbance peak for chlorophyll *a*.

radii will lead to a smaller number of cells per mass of bulk algae, and thus a smaller number of cells to split the heat load amongst.

Graham and Wilcox (2000) assert that *Chlorella* cells exist with radii between 1 and 6 microns. For the reversible case, there is little temperature rise along this range of radii, which seems a suitable indication that the amounts of heat that need to be rejected by the algae cells can feasibly be done so, as the algae cells are operating extremely close to ambient conditions. By contrast, in the irreversible case where average literature quantum requirement is used, the inner core temperatures approaches more noticeable temperature differences. While a temperature of just less than 27 °C at a cell radius of 6 microns is not unreasonable, species with larger cells might incur cell damage from higher core temperatures, which would imply that the average literature quantum requirement requires too large a rejection of heat, and thus that this quantum requirement value may be too high.

Chapter 3

Theoretical Biomass Growth Rates

3.1 Introduction and Approach

With the limit of operation for quantum requirement established, and a relevant mathematical model developed, attention can now be turned to the secondary objective of this dissertation. In determining the maximum theoretical amount of biomass that can be produced using energy from the sun, the aforementioned model will be utilised in conjunction with a model describing solar energy availability. In this sense, the upper limit of operation for biomass productivity can be set; this is the largest mass that, in theory, can be produced from the available light energy received from the sun.

Biomass growth rates are often reported in the units of g/m^2.day or g/m^2.hr: in other words, the mass grown per area per time. Thus for the purposes of this analysis, the area rate will be denoted by a dot above the relevant symbol. This notation is also relevant to energy flow of photons, $\dot{E}_{\text{photons}}$, which essentially reduces to W/m^2, as well as incoming photon density, $\dot{N}_{\text{photons}}$, in the units of mol photons/m^2.s.

In the previous analysis, the change in Gibbs free energy over the process was set to the Gibbs free energy of reaction, and thus the number of photons required to produce one mole of glucose was found. Here, the reverse procedure must now be applied: the number of available incoming photons must be utilised to determine the moles of glucose that can be produced. The number of photons received from the sun must be determined from a relevant and appropriate sources, and the issue raised in section 1.3.1.4 of percentage absorbance of these photons must also be incorporated into the analysis.

Establishing these figures will allow the total number of moles of glucose per area time to be calculated. Adjusting this to the conventional units of growth

rate is thus a matter of multiplying the number by the molecular weight of glucose; again, this serves to re-iterate the assumption of this dissertation that biomass is approximated wholly as glucose. This method of calculating theoretical biomass growth rates will be applied to two processes considered so far: (a) the reversible photosynthesis process with finite photon entropy that set the minimum limit of operation for quantum requirement, as concluded in the discussion of chapter 2; (b) the photosynthesis process that utilises the average literature quantum requirement, rejecting greater heat and being thermodynamically irreversible. These molar growth rates are indicated below:

$$\dot{N}_{\text{glucose,rev}} = \frac{\dot{N}_{\text{photons}}}{\text{QR}_{\text{glucose,rev}}} \tag{3.1.1}$$

$$\dot{N}_{\text{glucose,irrev}} = \frac{\dot{N}_{\text{photons}}}{\text{QR}_{\text{glucose,irrev}}} \tag{3.1.2}$$

The latter process is expected to result in a slower growth rate, since the number of photons it utilises to produce one mole of glucose is greater than that for the former process. It is also worth comparing these theoretical yields with actual, reported yields from experimental data. This will give an idea of how far the practical reality of growth by photosynthesis is from the theoretical possibilities.

3.2 Reversible Process

3.2.1 Total incident light

The quantum requirement for the reversible photosynthesis process with finite photon entropy is a function of wavelength, and ranges between 9.94 moles of photons at 400 nm and 17.8 moles at 700 nm, as determined in section 2.2.3. Thus, in addition to finding the number of photons received per area time, $\dot{N}_{\text{photons}}$, it is also required that a wavelength λ be set to establish a fixed value for the reversible quantum requirement value, $\text{QR}_{\text{glucose,rev}}$. Before determining how to set λ, the concepts and methods of finding the energy of the photons received per area time, $\dot{E}_{\text{photons}}$, and the number of photons received per area time, $\dot{N}_{\text{photons}}$, should be explored.

Both of these quantities can be related and obtained from the concept of spectral irradiance. Recall from section 1.3.3.2, the work and determination of spectral irradiance output, I, of a black body by Planck (1901). With

this variable, the amount of energy that the earth receives from the sun per area time can be approximated. Equation 1.3.4 quantifies the energy directly distributed by the sun, and thus the energy before encountering the earth's exosphere, or any physical matter. Substantial absorption and decay of light energy from atmospheric gas particles such as oxygen, nitrogen, water, carbon dioxide, and numerous others is a factor that must be considered.

In essence, Planck's equation, while being an effective approximation, does not represent the actual energy that a portion of land or sea would receive in reality. For a greater degree of accuracy, measured spectral irradiance should be considered. The American Society for Testing and Materials (ASTM, 2003) measures and provides the spectral irradiance at sea level, which is more useful and relevant to the task at hand, considering the location of biomass growth. This spectral irradiance is measured as an average of the quality of direct sunlight over the period of a year, and so takes into account changes in angle and amount of light received for a portion of land. Note that this data is specifically relevant to North American land areas.

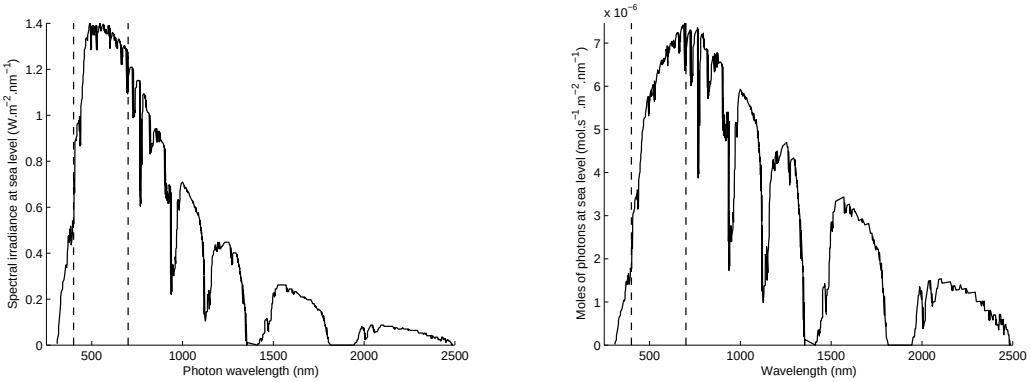
Figure 3.2.1a shows this spectral irradiance, with markers set for the photosynthetically active radiation range. If the area under the curve is calculated by integrating between 400 nm and 700 nm, the amount of energy received per unit area available to photosynthetic organisms can be found:

$$\dot{E}_{\text{photons}} = \int_{400\,\text{nm}}^{700\,\text{nm}} I.d\lambda \tag{3.2.1}$$

From the available data, this energy is found to be 376.1 W/m^2. The next issue is calculating the number of moles of photons received per area time. Since the spectral irradiance data, I, essentially represents the energy carried by incoming photons, this function can be divided by the definition for photon energy as a function of wavelength from equation 1.3.3. The result yields a curve describing the number of moles of photons per area time per wavelength, shown in figure 3.2.1b. Integrating this curve allows the incoming photon density to be calculated:

$$\dot{N}_{\text{photons}} = \int_{400\,\text{nm}}^{700\,\text{nm}} \frac{I\lambda}{N_A hc}.d\lambda \tag{3.2.2}$$

The incoming photon density is found to be 150.9 mol photons/m^2.day, or 1700 μmol photons/m^2.s. Therefore, both the energy of the photons received per area time, $\dot{E}_{\text{photons}}$, and the number of photons received per area time,



(a) Measured spectral irradiance. Data is sourced from the American Society for Testing and Materials (ASTM, 2003).

(b) Equivalent incoming photon density.

Figure 3.2.1: Measured solar irradiance (W/m^2.nm), shown in figure 3.2.1a, and equivalent incoming photon density (mol photons/m^2.s.nm), shown in figure 3.2.1b, at sea level with the photosynthetically active radiation (PAR) limits at 400 nm and 700 nm indicated by vertical dashed lines.

$\dot{N}_{\text{photons}}$, have been determined from data. This, however, does not resolve the issue of setting a wavelength λ and subsequently a fixed value for the reversible quantum requirement value, $\text{QR}_{\text{glucose,rev}}$.

A useful concept to introduce, therefore, is that of representative wavelength, λ_{rep}, which serves to correlate the entire photon density with one wavelength to match the energy flux. From the spectral irradiance data, both the energy of the photons, $\dot{E}_{\text{photons}}$, and the number of photons, $\dot{N}_{\text{photons}}$, are available. If the former is divided by the latter, the average energy of a photon can be estimated. Applying Planck's correlation for the energy of a photon (equation 1.3.3) allows calculation of the representative wavelength:

$$\lambda_{\text{rep}} = \frac{\dot{N}_{\text{photons}} N_{\text{A}} hc}{\dot{E}_{\text{photons}}} \tag{3.2.3}$$

The representative wavelength is calculated here to be 556nm. Thus, returning to the results shown in figure 2.2.2 of section 2.2.3, the quantum requirement for the reversible photosynthesis process with finite photon entropy can be given as 13.98 mol photons/mol glucose. Dividing the incoming photon density by this value, as demonstrated in equation 3.1.1, results in a theoretical growth rate of 81.0 g/m^2.hr of biomass, approximated as glucose.

3.2.2 Total absorbable light

The above growth rate is based upon the total spectral irradiance received by the earth within the photosynthetically active radiation spectrum. However, in reality, photosynthetic organisms can only use a portion of this, as defined by their action spectra. It makes sense to apply the light absorbance of each wavelength in the PAR spectrum to arrive at the total light absorbed by an organism and a more realistic calculated growth rate. Thus, recall figure 1.3.2 from section 1.3.1.4, and reconsider the definition of percentage absorbance:

$$A_\lambda = \frac{\text{Total light absorbed for } \lambda}{\text{Total light received for } \lambda} \times 100$$

Only a portion of the photons received, and therefore the energy flux, at each wavelength λ will be absorbed according to the value of A_λ. It is simple to apply this to equations 3.2.1and 3.2.2 to yield the following:

$$\dot{E}_{\text{photons,abs}} = \int_{400\text{ nm}}^{700\text{ nm}} A_\lambda I.d\lambda \tag{3.2.4}$$

$$\dot{N}_{\text{photons,abs}} = \int_{400\text{ nm}}^{700\text{ nm}} \frac{A_\lambda I\lambda}{N_A hc}.d\lambda \tag{3.2.5}$$

Note that the percentage absorbance values utilised here from figure 1.3.2, as provided by Whitmarsh and Govindjee (1999), are relevant only to chlorophyll *a*. The abundance of chlorophyll *a* in natural organisms makes the usage of this data appropriate. The calculated energy flux for the total absorbable light, $\dot{E}_{\text{photons,abs}}$, is thus calculated to be 92.67W/m^2. The calculated absorbed photon density, $\dot{N}_{\text{photons,abs}}$, is calculated to be 36.37 mol photons/m^2.day, or 420.1 μmol photons/m^2.s.

However, before dividing the absorbed photon density with the quantum requirement for the reversible photosynthesis process with finite photon entropy previously used for 556 nm, the above adjusted energy and photon flux terms should be examined. The nature of the action spectrum of chlorophyll *a*, and therefore the percentage absorbance of each wavelength, does not simply allow $\dot{E}_{\text{photons}}$ and $\dot{N}_{\text{photons}}$ to be scaled down to $\dot{E}_{\text{photons,abs}}$ and $\dot{N}_{\text{photons,abs}}$ by a common constant. Chlorophyll *a* favours red and blue light absorption in particular, and some wavelengths are hardly absorbed at all. Thus, a new representative wavelength, $\lambda_{\text{rep,abs}}$, will need to be calculated. Equation 3.2.3

can be altered to obtain:

$$\lambda_{\text{rep,abs}} = \frac{\dot{N}_{\text{photons,abs}} N_{\text{A}} hc}{\dot{E}_{\text{photons,abs}}} \tag{3.2.6}$$

Thus, based on the percentage absorbance data for chlorophyll *a,* the representative wavelength for the total absorbed light is 543nm. Again, returning to the results shown in figure 2.2.2 of section 2.2.3, the quantum requirement for the reversible photosynthesis process with finite photon entropy can be given as 13.65 mol photons/mol glucose at this wavelength. Dividing the absorbable incoming photon density by this value results in a theoretical growth rate of 20.0 g/m^2.hr of biomass or glucose.

3.3 Irreversible Process

3.3.1 Total incident light

The next growth rate to be considered is the theoretical maximum if the average literature quantum requirement, $\text{QR}_{\text{glucose,irrev}}$, is utilised. In this case, according to the model developed, the process is not using the minimum amount of photons to satisfy the reaction reversibly, but is instead using an excess number of 61.7 mol photons/mol glucose to synthesise the reaction. With the increased heat rejection and internal entropy generated, this makes this process scenario an irreversible one.

The calculation of the theoretical biomass growth rate for the irreversible process is far simpler as its quantum requirement has already been specified. For the case of utilising the total spectral irradiance received at sea level, the incoming photon density, $\dot{N}_{\text{photons}}$, is 150.9 mol photons/m^2.day, as calculated previously. Therefore, by way of equation 3.1.2, the theoretical maximum growth rate for the average literature quantum requirement for this scenario is calculated to be 18.4 g/m^2.hr.

3.3.2 Total absorbable light

As above, the average literature quantum requirement, $\text{QR}_{\text{glucose,irrev}}$, remains as 61.7 mol photons/mol glucose. However, the incoming photon density is reduced to a value of 36.37 mol photons/m^2.day, according to the percentage absorbance of light for chlorophyll *a*, as was calculated in section 3.3.2. The theoretical maximum growth rate for the average literature quantum require-

ment for the amount of absorbable light by chlorophyll a is calculated to be $4.42\,\mathrm{g/m^2.hr}$.

3.4 Photosynthetic Efficiency

The concept of photosynthetic efficiency that was introduced in section 1.3.5 is now returned to, as it is of interest in comparing theoretical and measured growth rates. In the case of the theoretical reversible and irreversible growth rates, it is also interesting to examine how each differs when considering the potential for growth from the total light energy in the photosynthetically active radiation spectrum (400 nm to 700 nm), as well as the potential from the absorbable light in this region.

Generally, the photosynthetic efficiency can be described as:

$$\eta = \frac{\text{Light energy used to produce biomass}}{\text{Total light energy received}}$$

This can be mathematically interpreted as:

$$\eta = \frac{\dot{N}_{\text{glucose}} \times \Delta G^{\circ}_{\text{rxn}}}{\dot{E}_{\text{photons}}}$$

Here, $\dot{N}_{\text{glucose}}$ is indeed the growth rate, specified as the number of moles of glucose produced per area per time (mol glucose/$\mathrm{m^2}$.s). $\Delta G^{\circ}_{\text{rxn}}$ is the Gibbs free energy required to synthesise one mole of glucose from the reactants of carbon dioxide and water, given as energy per mole (kJ/mol glucose). $\dot{E}_{\text{photons}}$ is the calculated total solar energy received by the photosynthetic system, derived from the spectral irradiance curve provided above by the ASTM (2003), given in units of energy per area per time ($\mathrm{W/m^2}$).

What is important to note is that this efficiency here is defined always with regard to the total and complete light energy available to the organisms, not merely the absorbable light. Therefore, because of the natural action spectra of such pigments, the efficiency will always be substantially lower than 100%, since a large majority of the light energy between 400 nm and 700 nm cannot be absorbed by the organism.

3.5 Results

The theoretical growth rates, both reversible and irreversible, estimated are all calculated in the units of g/m^2.hr using both the total spectral irradiance of direct sunlight in the photosynthetically active radiation spectrum, as well as the absorbable portion of light in this range, as has been described earlier. For the sake of accurate comparison, rates of biomass growth from experimental literature must be represented on a similar time-scale.

Fortunately, carbon dioxide uptake and oxygen evolution rates are often measured as hourly rates in direct sunlight. Moss (1967) supplies the maximum rate of carbon dioxide uptake per leaf area by crops in direct sunlight, and Doucha et al. (2005) supply the rate of oxygen evolution by algae per area of algal culture in direct sunlight. Both species are good examples of fast and effective growing photosynthetic organisms. In a different manner, Goudriaan and van Laar (1994) provide carbon dioxide uptake rates as a mass per joule of light energy absorbed.

Where attention should be raised is that the total spectral irradiance values given by the ASTM (2003) represent the average light received by a portion of land over a year. This includes various conditions where less light energy than that possessed by direct sunlight would be available: early mornings, late afternoons, cloudy or rainy days etc. This is a point to be have in mind when comparing theoretical growth rates, using an average hourly scale over a year, to measured growth rates, where light conditions would be favourable: direct, unobstructed sunlight.

The next concept to be discussed is that of reaction rate. In the simplified analysis of carbon dioxide, oxygen, water and glucose, relevant information from the literature review on light-dependent and light-independent reactions (sections 1.3.1.2 and 1.3.1.3, respectively) can be brought into use. It is conclusive from this review that the reaction or production rates of oxygen, $\dot{N}_{O_2}$ (mol/m^2.hr), and glucose, $\dot{N}_{\text{glucose}}$ (mol/m^2.hr), cannot simply be related by the stoichiometry of equation 1.3.2. The same can be said in the comparison of the oxygen evolution rate and the carbon dioxide uptake rate, $\dot{N}_{CO_2}$ (mol/m^2.hr). This is because the light-dependent reactions, which produce oxygen, occur at greater rates than the light-independent reactions, which consume carbon dioxide and produce glucose. In addition to this, there are the issues of cellular respiration and photorespiration, which hamper growth, even though the light-dependent reactions continue to proceed.

Representing this mathematically:

$$|\dot{N}_{O_2}| \geq |\dot{N}_{CO_2}|$$

$$\therefore |\dot{N}_{O_2}| \geq |6\dot{N}_{glucose}|$$

This is of importance for the measured growth rates provided. In the case of Doucha et al. (2005), the rate of oxygen evolution is provided. However, the molar rate of biomass production will not simply be one-sixth of this rate. The molar rate of carbon dioxide uptake will also not equal the oxygen evolution rate. In essence, it is possible to calculate a biomass growth rate and carbon dioxide uptake rate for the data provided by Doucha et al. (2005) from stoichiometry, but these would be the absolute maximums attainable based on the oxygen evolution rate.

Doucha et al. (2005) state that oxygen can be evolved photosynthetically at a rate of 7.1 g/m^2.hr of algal culture area. Thus, the maximum possible carbon dioxide uptake would be 9.8 g/m^2.hr, and the maximum possible biomass growth rate would be 6.7 g/m^2.hr. The assumption made here is that because carbon dioxide and glucose are directly related in the light-independent reactions, the rates of carbon dioxide uptake and glucose production can be stoichiometrically related as:

$$|\dot{N}_{CO_2}| \approx |6\dot{N}_{glucose}|$$

It would be safer to say that the glucose or biomass production rate is the maximum achievable, in case the carbon dioxide uptake and glucose production rates cannot be approximated by stoichiometry, though.

On the contrary, if a carbon dioxide uptake rate has been given, as in the case of Moss (1967) and Goudriaan and van Laar (1994), then an equivalent biomass production rate can be calculated, as well as the minimum oxygen evolution rate. In reality, it is possible for the oxygen evolution rate to be greater than the calculated one, owing to the faster kinetics of the light-dependent reactions. Moss (1967) asserts that the maximum carbon dioxide uptake rate in corn is approximately 6.0 g/m^2.hr of leaf area. To illustrate the above, the corresponding minimum oxygen evolution rate would be 4.4 g/m^2.hr, and the approximate maximum biomass growth rate would be about 4.1 g/m^2.hr.

Goudriaan and van Laar (1994) state that between 11μg and 14μg of carbon dioxide are absorbed in plants for every joule of light received. Thus, basing the received light on the figure calculated for the absorbable light in section

Model/Biomass type	Carbon dioxide uptake rate ($g/m^2.hr$)	Oxygen evolution rate ($g/m^2.hr$)	Maximum biomass rate ($g/m^2.hr$)
Total light, reversible	119	86.3	81.0
Absorbable light, reversible	29.3	21.3	20.0
Total light, irreversible	27.0	19.6	18.4
Absorbable light, irreversible	6.48	4.71	4.42
Algae (Doucha et al., 2005)	9.8 (Maximum)	7.1 (Given)	6.7 (Maximum)
Crops (Moss, 1967)	6.0 (Given)	4.4 (Minimum)	4.1 (Maximum)
C-4 plants(Goudriaan and van Laar, 1994)	6.8 (Given)	5.0 (Minimum)	4.7 (Maximum)

Table 3.5.1: Summary of theoretical and literature-based rates of carbon dioxide uptake, oxygen evolution, and maximum biomass generation. The reversible rates utilise the theoretical quantum requirement in the minimum limit of operation scenario, while the irreversible rates utilise the average literature quantum requirement. The measured rates are given for oxygen evolution in the case of Doucha et al. (2005), and for carbon dioxide uptake by Moss (1967) and Goudriaan and van Laar (1994). The stoichiometrically equivalent biomass rates are the maximum possible, but not necessarily realistically attainable, due to reaction kinetic differences and inefficiencies.

3.3.2, $92.67 W/m^2$, this yields a carbon dioxide uptake rate of $6.8\ g/m^2.hr$. The corresponding maximum rate of biomass production would be $4.7\ g/m^2.hr$, and the minimum rate of oxygen evolution would be $5.0\ g/m^2.hr$.

The theoretical calculations calculated in section 3.2.1 through to section 3.3.2 can now be compared with the measured experimental values. The values of the growth rates are summarised and available in table 3.5.1. Note that for the theoretically calculated biomass growth rates, the corresponding oxygen evolution and carbon dioxide uptakes rates have been calculated by simple stoichiometry. Of greatest importance is to compare the biomass growth rates; it was therefore necessary to utilise oxygen and carbon dioxide rates from literature to arrive at estimable biomass growth rates.

The first observation is that the theoretically calculated rates for the reversible and irreversible process utilising the full spectral irradiance in the PAR spectrum are significantly higher than those calculated when applying the absorbance capabilities of chlorophyll *a*. In both the reversible and irreversible processes, the biomass growth rate is approximately 4 times the absorbable light value when using the entire energy available in the photosynthetically

Model/Biomass type	Photosynthetic efficiency (%)
Total light, reversible	95.7
Absorbable light, reversible	23.6
Total light, irreversible	21.7
Absorbable light, irreversible	5.22
Algae (Doucha et al., 2005)	7.9
Crops (Moss, 1967)	4.8
C-4 plants (Goudriaan and van Laar, 1994)	5.6

Table 3.5.2: Photosynthetic efficiences calculated from the biomass growth rates in table 3.5.1, and based upon the total amount of light received in the photosynthetically active radiation spectrum of 400 nm to 700 nm.

active radiation spectrum. Interestingly, in the case of utilising only the absorbable amount of light, the absorbable photon density was calculated from the data provided by the ASTM (2003) and Whitmarsh and Govindjee (1999) to be 420.1 μmol photons/m^2.s. This value corresponds well to the agreement by Tsuyama et al. (2003) and Melis (2009) that light saturation of the photosynthetic process occurs at approximately 400 μmol photons/m^2.s.

Examining the concept of photosynthetic efficiency, with a summary of all the calculated efficiencies available in table 3.5.2, the reversible process utilising all available light is able to achieve an efficiency of 95.7%. In essence, this implies that 95.7% of the available light could be converted to chemical energy in the form of biomass. As discussed in section 2.3.2, even the reversible process must reject heat to the environment, thus accounting for the 4.3% efficiency lost. If only the absorbable portion of light is used for calculation, then this efficiency is dramatically lowered to 21.7%. Thus, the light saturation effect can be considered a major factor in reducing the total potential for biomass growth, as all the light energy available is simply not utilised.

In comparing the reversible and irreversible values of biomass growth calculated, the reversible growth rate is greater than 4 times the irreversible biomass growth rate. This can be explained by the greater quantum requirement of the irreversible process (61.7 mol photons/mol glucose) in comparison to that of the reversible process (between 13.65 mol photons/mol glucose and 13.98 mol photons/mol glucose in the calculations of this chapter). In both the total available light and absorbable light scenarios, this is the case. Noticeably, the photosynthetic efficiency drops greatly when comparing the irreversible cases to the reversible ones. This indicates the inefficiency of the irreversible

process, as much of the input light energy is rejected as heat.

If the average literature quantum requirement is used to predict growth rate for only the absorbable amount of light energy, then this results in an average biomass growth rate of 4.42 g/m^2.hr and a photosynthetic efficiency of 5.22%. An intriguing observation here is that the maximum calculated biomass growth rates of Doucha et al. (2005) and Goudriaan and van Laar (1994) in direct sunlight exceed this theoretical rate, which would initially imply that the average literature quantum requirement is to be questioned.

However, three explanations can be offered here to resolve this point. Firstly, as mentioned earlier, the theoretical rates are calculated on an average hourly rate from spectral irradiance data over a year, as opposed to experimental rates, which would most likely use direct sunlight. Thus, the theoretical growth rate may be larger if calculated with the irradiance from one actual hour of direct, bright sunlight of favourable conditions. Secondly, the maximum calculated biomass growth rates for Doucha et al. (2005) and Goudriaan and van Laar (1994) are based on the oxygen evolution and the carbon dioxide uptake rate, respectively. In reality, these rates would be faster than the stoichiometrically-related carbon or biomass fixation rates.

This is particularly the case with the oxygen evolution rate of Doucha et al. (2005), considering the superior kinetics of the light-dependent reactions to the light-independent reactions, as well as any occurrences of cellular respiration and photorespiration. It may be less so the case with the carbon dioxide uptake rate of Goudriaan and van Laar (1994). However, there may still be factors in the light-independent reactions that reduce the biomass production rate such that it cannot be calculated to be the exact stoichiometrical equivalent of the carbon dioxide uptake rate. Therefore the actual, as opposed to the maximum possible, biomass growth rates for both measured sources are likely to be lower than those calculated here.

A third explanation regards the quantum requirement value used in the calculation for irreversible process. From the literature review in section 1.3.4, measured quantum requirement values range between 36 and 75 moles of photons per mole of glucose, with an average value used in the growth rate calculations here of 61.7 moles of photons per mole of glucose. It is possible therefore that with a lower measured quantum requirement, the calculated biomass growth rate for the irreversible process would exceed the maximum biomass growth rates for Doucha et al. (2005) and Goudriaan and van Laar (1994).

For the results provided by Moss (1967), the maximum possible biomass growth rate is lower than the reversible and irreversible theoretical ones. The carbon dioxide uptake rate of Moss (1967) is used to calculate stoichiometrically related biomass growth rate. Again, this is the maximum possible, not necessarily the biomass growth rate obtained in reality.

The calculated photosynthetic efficiencies from experimental values vary between 4.8% (Moss, 1967) and 7.9% (Doucha et al., 2005). These values correspond well with the predicted efficiences by Andriesse and Hollestelle (2001). Despite this, the efficiencies are still low, considering the total amount of solar energy that is available to photosynthetic organisms. It is necessary now to examine what may be causing discrepancies between theoretical and measured growth rates. This brings to relevance discussion of the inner workings of the photosynthetic process, and more specifically the limiting factors in the light-dependent and light-independent reactions.

3.6 Discussion

Of immediate concern, demonstrated by the above results, is the large difference between theoretical growth rates, regardless of quantum requirement, from total available light and absorbable light. The unfortunate effect of this is that so much potential growth, indicated by the severely lowered photosynthetic efficiency, is lost because the oxygen evolution and ATP and NADPH generation reactions reach a plateau as a result of light saturation. It is a combination of limiting factors in both the light-dependent reactions and light-independent reactions that causes this.

In the light-dependent reactions, it is the slow binding of plastoquinone to appropriate sites on the Cytochrome c6f complex which causes a bottleneck (Govindjee and Govindjee, 2000). The slowness of this binding is accountable to the lack of availability of such sites (Whitmarsh and Govindjee, 1999). The electrons that are rapidly delivered from photoexcited reaction centre P680 are therefore limited in their movement to the next reaction centre by this restriction. In the light-independent reactions, the Rubisco enzyme possesses a similar problem of only being able to bind carbon dioxide molecules to its available sites at an even slower rate (Tcherkez et al., 2006). The uptake of oxygen molecules by Rubisco instead of carbon dioxide molecules for photorespiration further reduces its efficiency and rate of carbon fixation (Parry et al., 2003).

In the combined effect of these bottlenecks, it is ultimately the Rubisco enzyme which limits the photosynthetic rate from an overall perspective. The Cytochrome c6f complex works slowly, but can deliver – along with the rest of the electron transport chain – sufficient ATP and NADPH to the stroma side of the thykaloid membrane. The Rubisco enzyme cannot, however, deliver products at the rate at which it receives its necessary reactants.

The light saturation effect therefore provides adequate explanation as to why there is such a large difference between the growth rates that could in theory utilise all available light energy and those that could only use the absorbable amount of such energy. However, there are still discrepancies between the theoretical values utilising only the absorbable light energy and measured growth rates. Attention can now be turned to this discussion.

Relevant factors that limit physical biomass growth rates include cellular respiration and photorespiration (Forrester et al., 1966), which directly undermine biomass growth by consuming the carbon-based products of photosynthesis. The latter process favours high-oxygen, low-carbon dioxide environments, making atmospheric conditions ideal for it to occur. Melis (2009) suggests that these two factors may reduce the overall rate of biomass growth by about 30%.

An additional factor that may contribute to discrepancies between theoretical growth rates and the actual, realistic ones obtained experimentally in literature is the issue of reactant availability. The point is made by van Hunnik et al. (2000) that aquatic photosynthetic organisms, such as microalgae, whilst having access to surplus amounts of water, can have their growth rates limited by carbon dioxide availability. This may also be an issue for organisms securing carbon dioxide from the atmosphere, which encompasses a large variety of plants, considering that the concentration of carbon dioxide in relation to oxygen and nitrogen is low in air.

While this analysis simplifies the requirements of biomass growth to carbon dioxide and water, there are many other elements and nutrients necessary to stimulate the growth process (Beadle and Long, 1985). For example, the magnesium ion is a central component in chlorophyll molecules; without a supply of this element, chlorophyll cannot be formed and photosynthesis cannot perpetuate.

The point of illustrating some of these factors is to indicate the wide number of factors that limit physical biomass growth. In this way, they can, to an extent, account for differences between theoretically calculated and physically possible growth rates. The benefit of having determined the maximum theo-

retical growth rates lies in that the upper constraint on biomass production from photosynthesis has been set.

Thus, with available solar energy, one can quantify biomass generation with varying efficiencies in comparison to the absolute maximum that is possible: the growth rate based on the perfectly reversible, theoretical process. With the total light available in the PAR spectrum, this amount is therefore $81.0 g/m^2.hr$ of biomass, approximated as glucose.

Chapter 4

Conclusions and Recommendations

The reversible quantum requirement for the photosynthetic process determined in this work is substantially less than the quantum requirements provided by literature, which are experimentally measured values. The usefulness of the reversible quantum requirement is that it sets the limit of operation for a potential photosynthetic process, natural or artificial. In essence, this is the very best performance that a reversible process could produce in terms of solar energy utilisation: it is the minimum number of photons required for glucose synthesis, if the process operates with the greatest thermodynamic efficiency.

If the average literature quantum requirement is placed into the equations of the thermodynamic model of this dissertation, then an internal entropy generation term, S_{gen}, is necessary to satisfy these equations. This would imply that the photosynthetic process is largely irreversible, and that natural organisms do not utilise photon energy effectively. If these experimental quantum requirement values are correct, then opportunity to improve and optimise reversibility is available.

Another important conclusion from the thermodynamic model is that, regardless of the degree of reversibility, the process must reject heat to the surroundings. By considering a basic heat rejection model, the difference between the amount of heat rejected by the reversible and irreversible processes can be demonstrated. The results of this model are not compelling enough to conclude which quantum requirement is the correct one, but is a useful tool nonetheless.

A major result of the comparison between theoretical and measured growth rates of photosynthetic organisms is the demonstration that much potential for growth is lost due to the fact that not all light in the photosynthetically active

radiation spectrum can be utilised. Again, considering the reversible quantum requirement and the total available light between 400 nm and 700 nm a limit of operation has been set. This is the maximum amount of biomass that can be grown with the light available by a thermodynamically efficient photosynthetic process within in this wavelength range.

To improve the conversion efficiency of the solar energy available to photosynthetic organisms, improvements in the cell's biology are required as to remove bottlenecks, thus eliminating the light saturation effect. As indicated by Whitmarsh and Govindjee (1999), the Cytochrome c6f complex has limited binding sites for plastoquinone molecules. A recommendation here might be to genetically alter the number of sites on such a protein, or to have more such complexes per cell, so that the plastoquinone molecules are processed as fast as they are received by the complex.

In the case of the Rubisco enzyme, a great deal of research has been directed to similar methods of genetic modification. Increasing the amount of Rubisco found in plant cells would improve the rate at which carbon dioxide could be processed (Parry et al., 2003). Increasing the specificity of carbon dioxide uptake to oxygen uptake by the enzyme would reduce photorespiration and improve carbon fixation, growth rate and overall photosynthetic performance (Andrews and Whitney, 2003). Interestingly, however, Rachmilevitch et al. (2004) make the suggestion that photorespiration serves a valuable purpose in the assimilation of nitrates, which are useful nutrients in the growth and structuring of a various plants, and thus that such genetic alterations may be harmful in this regard.

The above are only a few relevant points in the field of genetic modification for photosynthetic organisms, which is wide and detailed, and deserves more attention than can be summarised here. Ultimately, the hope with such modifications is the improved efficiency of the photosynthetic process. By doing so, larger amounts of biomass can be grown faster in comparison to amounts grown currently, and thus accommodate the requirements of the biofuels, agricultural and various other industries.

Bibliography

Alberty, R. A., 1998. Calculation of standard transformed Gibbs energies and standard transformed enthalpies of biochemical reactants. Biochemistry and Biophysics 353, 116–130.

Andrews, T. J., Whitney, S. M., 2003. Manipulating ribulose bisphosphate carboxylase/oxygenase in the chloroplasts of higher plants. Archives of Biochemistry and Biophysics 414, 159–169.

Andriesse, C. D., Hollestelle, M. J., 2001. Minimum entropy production in photosynthesis. Biophysical Chemistry 90, 249–253.

ASTM, 2003. American society for testing and materials terrestrial reference spectra for photovoltaic performance evaluation.
URL `http://rredc.nrel.gov/solar/spectra/am1.5/`

Beadle, C. L., Long, S. P., 1985. Photosynthesis - is it limiting to biomass production? Biomass 8, 119–168.

Berg, J. M., Tymoczko, J. L., Stryer, L., 2002. Biochemistry, 5th Edition. W. H. Freeman, New York.

Bird, R. B., Stewart, W. E., Lightfoot, E. N., 2002. Transport Phenomena. John Wiley & Sons, Inc.

Björkman, O., Demmig, B., 1987. Photon yield of oxygen evolution and chlorophyll fluorescence characteristics at 77 K among vascular plants of diverse origins. Planta 170, 489–504.

Brown, T. L., LeMay, H. E., Bursten, B. E., Burdge, J. R., 2002. Chemistry: The Central Science, 9th Edition. Prentice Hall.

Bryant, D. A., Frigaard, N.-U., 2006. Prokaryotic photosynthesis and phototrophy illuminated. Trends in Microbiology 14, 488–496.

Burlew, J. S., 1953. Algal Culture: From Laboratory to Pilot Plant. Carnegie Institution of Washington Publication, Ch. 1: Current status of the large-scale culture of algae, pp. 3–23.

Chain, R. K., Arnon, D. I., 1977. Quantum efficiency of photosynthetic energy conversion. Proc. Natl. Acad. Sd. 74, 3377–3381.

Chisti, Y., 2007. Biodiesel from microalgae. Biotechnology Advances 25, 294–306.

Demirbas, A., 2009. Biofuels securing the planet's future energy needs. Energy Conversion and Management 50, 2239–2249.

Doucha, J., Straka, F., Lívanský, K., 2005. Utilization of flue gas for cultivation of microalgae (Chlorella sp.) in an outdoor open thin-layer photobioreactor. Journal of Applied Phycology 17, 403–412.

Energy Aquatic Species Program, U. S., 2006. Biodiesel production from algae. Tech. rep., US Department of Energy Aquatics Species Program.

Field, C. B., Behrenfeld, M. J., Randerson, J. T., Falkowski, P., 1998. Primary production of the biosphere: integrating terrestrial and oceanic components. Science 281, 237–240.

Forrester, M. L., Krotkov, G., Nelson, C. D., 1966. Effect of oxygen on photosynthesis, photorespiration and respiration in detached leaves. i. soybean. Plant Physiology 41, 422–427.

Fragata, M., Viruvuru, V., 2008. Quantum requirement for oxygen evolution in photosystem II: new experimental data and theoretical solutions. In: Allen, J. F., Gantt, E., Golbeck, J. H., Osmond, B. (Eds.), Photosynthesis. Energy from the Sun: 14th International Congress on Photosynthesis. Springer, pp. 401–404.

Goudriaan, J., van Laar, H. H., 1994. Modelling potential crop growth processes. Kluwer Academic Publishers, Dordrecht, The Netherlands.

Govindjee, 1999. On the requirement of minimum number of four versus eight quanta of light for the evolution of one molecule of oxygen in photosynthesis: A historical note. Photosynthesis Research 59, 249–254.

Govindjee, Govindjee, R., November 2000. Photosynthesis and the "Z"-scheme.
URL http://www.life.uiuc.edu/govindjee

Govindjee, R., Rabinowitch, E., Govindjee, 1968. Maximum quantum yield and action spectrum of photosynthesis and fluorescence in Chlorella. Biochimica et Biophysica Acta 162, 539–544.

Graham, L. E., Wilcox, L. W., 2000. Algae. Prentice Hall.

Gudkov, N. D., 1998. Some thermodynamics of chemiluminescence. Journal of Luminescence 79, 85–89.

Jeong, M. L., Gillis, J. M., Hwang, J.-Y., 2003. Carbon dioxide mitigation by microalgal photosynthesis. Bull. Korean Chem. Soc. 24, 1763–1766.

Jones, M. R., Fyfe, P. K., 2004. Photosynthesis: a new step in oxygen evolution. Current Biology 14, 320–322.

Kahn, D., 1961. A note on efficiency of photon absorption. Plant Physiology 36, 539–540.

Kalyanasundaram, K., Graetzel, M., 2010. Artificial photosynthesis: biomimetic approaches to solar energy conversion and storage. Current Opinion in Biotechnology 21, 298–310.

Karnaukhov, A. V., 2001. Role of the biosphere in the formation of the earth's climate: the greenhouse catastrophe. Biophysics 46, 1138–1149.

Karube, I., Takeuchi, T., Barnes, D. J., 1992. Biotechnological reduction of carbon dioxide emissions. Advances in Biochemical Engineering/Biotechnology 46, 63–79.

Kirwan, A. D., 2004. Intrinsic photon entropy? the darkside of light. International Journal of Engineering Science 42, 725–734.

Leff, H. S., 2002. Teaching the photon gas in introductory physics. Am. J. Phys. 70, 792–797.

Ley, A. C., 1986. Relationships among cell chlorophyll content, photosystem II light-harvesting and the quantum yield for oxygen production Chlorella. Photosynthesis Research 10, 189–196.

Ley, A. C., Mauzerall, D. C., 1982. Absolute absoprion cross-sections for photosystem II and the minimum quantum requirement for photosynthesis in Chlorella vulgaris. Biochimica et Biophysica Acta 680, 95–106.

Lineweaver, C. H., Egan, C. A., 2008. Life, gravity and the second law of thermodynamics. Physics of Life Reviews 5, 225–242.

Listorti, A., Durrant, J., Barber, J., 2009. Artificial photosynthesis - solar to fuel. Nature Materials 8, 929–930.

Melis, A., 2009. Solar energy conversion efficiencies in photosynthesis: minimizing the chlorophyll antennae to maximize efficiency. Plant Science 177, 272–280.

Moss, D. N., 1967. Solar energy in photosynthesis. Solar Energy 11, 173–179.

Myers, J., 1953. Algal Culture: From Laboratory to Pilot Plant. Carnegie Institution of Washington Publication, Ch. Growth Characteristics of Algae in Relation to the Problems of Mass Culture, pp. 37–54.

Nabors, M. W., 2004. Introduction to Botany. Pearson Education Inc., San Francisco, California.

Ogbonna, J. C., Yada, H., Tanaka, H., 1995. Kinetic study on light-limited batch cultivation photosynthetic cells. Journal of Fermentation and Bioengineering 80, 259–264.

Parry, M. A. J., Andralojc, P. J., Mitchell, R. A. C., Madgwick, P. J., Keys, A. J., 2003. Manipulation of Rubisco: the amount, activity, function and regulation. Journal of Experimental Botany 54 (386), 1321–1333.

Patel, B., Hildebrandt, D., Glasser, D., Hausberger, B., 2005. Thermodynamics analysis of processes: 1. Implications of work integration. Ind. Eng. Chem. Res. 44, 3529.

Petela, R., 2008. An approach to the exergy analysis of photosynthesis. Solar Energy 82, 311–328.

Planck, M., 1901. On the law of distribution of energy in the normal spectrum. Annalen der Physik 4, 553.

Rachmilevitch, S., Cousins, A. B., Bloom, A. J., 2004. Nitrate assimilation in plant shoots depends on photorespiration. Proceedings of the National Academy of Sciences of the United States of America 101 (31), 11506–11510.

Ragauskas, A. J., Williams, C. K., Davison, B. H., Britovsek, G., Cairney, J., Eckert, C. A., Jr., W. J. F., Hallett, J. P., Leak, D., Liotta, C. L., Mielenz, J. R., Murphy, R., Templer, R., Tschaplinski, T., 2007. The path forward for biofuels and biomaterials. Science 311, 484–489.

SARDI, 2008. Microalgal production. Tech. rep., SARDI Aquatic Sciences, Government of South Australia, Henley Beach, South Australia.

Schmid, G. H., Gaffron, H., 1967. Quantum requirement for photosynthesis in chlorophyll-deficient plants with unusual lamellar structures. The Journal of General Physiology 50, 2131–2144.

Shinkarev, V. P., 2003. Oxygen evolution in photosynthesis: simple analytical solution for the Kok model. Biophysical Journal 85, 435–441.

Spoehr, H. A., 1953. Algal Culture: From Laboratory to Pilot Plant. Carnegie Institution of Washington Publication, Ch. 2: The need for a new source of food, pp. 24–28.

Taiz, L., Zeiger, E., 2010. Plant physiology online: a companion to plant physiology, fifth edition.
URL `5e.plantphys.net`

Tcherkez, G. G. B., Farquhar, G. D., Andrews, T. J., 2006. Despite slow catalysis and confused substrate specificity, all ribulose bisphosphate carboxylases may be nearly perfectly optimized. Proceedings of the National Academy of Sciences of the United States of America 103 (19), 7246–7251.

Tsuyama, M., Shibata, M., Kobayashi, Y., 2003. Leaf factors affecting the relationship between chlorophyll fluorescence and the rate of photosynthetic electron transport as determined from CO2 uptake. J. Plant Physiol. 160, 1131–1139.

van Hunnik, E., van den Ende, H., Timmermans, K. R., Laan, P., de Leeuw, J. W., 2000. A comparison of CO2 uptake by the green algae Tetraedron minimum and Chlamydomonas monoica. Plant biol. 2, 624–627.

Warburg, O., Krippahl, G., Lehman, A., 1969. Chlorophyll catalysis and Einstein's law of photochemical equivalence in photosynthesis. Am. J. Bot. 56, 961–971.

Warner, J. W., Berry, R. S., 1987. Alternative perspective on photosynthetic yield and enhancement. Proc. Natl. Acad. Sci. 84, 4103–4107.

Whitmarsh, J., Govindjee, 1999. Concepts in Photobiology: Photosynthesis and Photomorphogenesis. Narosa Publishers, New Delhi, Ch. The Photosynthetic Process, pp. 11–51.

Whitney, S. M., Andrews, T. J., 2001. Plastome-encoded bacterial ribulose-1,5-bisphosphate carboxylase/oxygenase (RubisCO) supports photosynthesis and growth in tobacco. Proceedings of the National Academy of Sciences of the United States of America 98 (25), 14738–14743.

Yourgrau, W., van der Merwe, A., March 1968. Entropy balance in photosynthesis. Proceedings of the National Academy of Sciences of the United States of America 59 (3), 734–737.

Zeinalov, Y., Maslenkova, L., 1999. Estimation of the quantum efficiency of photonsynthesis. I. Theoretical ground and experimental approaches. Bulg. J. Plant Physiol. 25, 26–38.

Appendix A

Linking Irreversibility and Heat Rejection

While the number of photons required to synthesise one mole of glucose (or one mole of reaction) is described by equation 2.1.10, a link between the internal entropy generated in the photosynthesis system, S_{gen}, and the heat rejected by the system to the surroundings, Q, is to be made here. Beginning with the entropy balance derived in section 2.1.2:

$$S_{\text{in}} + S_{\text{gen}} + S_{\text{photons}} = S_{\text{out}} + \frac{Q}{T}$$

Rearranging this:

$$Q = TS_{\text{gen}} + TS_{\text{photons}} + TS_{\text{in}} - TS_{\text{out}}$$

With the knowledge that:

$$\Delta S_{\text{process}} = S_{\text{out}} - S_{\text{in}}$$

The equation reduces to:

$$Q = TS_{\text{gen}} + TS_{\text{photons}} - T\Delta S_{\text{process}}$$

Now, if the entropy change over the process is defined with respect to the enthalpy and Gibbs free energy changes over the process, the following is obtained:

$$\Delta G_{\text{process}} = \Delta H_{\text{process}} - T\Delta S_{\text{process}}$$

Thus, by substituting this definition into the main equation:

$$Q = TS_{\text{gen}} + TS_{\text{photons}} + \Delta G_{\text{process}} - \Delta H_{\text{process}}$$

The entropy of photons term is now expanded by inserting equation 2.1.4:

$$Q = TS_{\text{gen}} + T\left(N_{\text{photons}} N_{\text{A}} \hat{S}_{\text{photon}}\right) + \Delta G_{\text{process}} - \Delta H_{\text{process}}$$

The aforementioned, primary equation to describe quantum requirement is now substituted into this equation to replace the N_{photons} term:

$$Q = TS_{\text{gen}} + T\hat{S}_{\text{photon}} \left[\frac{\Delta G_{\text{process}} + T_{\text{o}} S_{\text{gen}}}{\left(\frac{hc}{\lambda} - T_{\text{o}} \hat{S}_{\text{photon}}\right)} \right] + \Delta G_{\text{process}} - \Delta H_{\text{process}}$$

The above equation is therefore able to express the heat rejected from the system as a function of variables S_{gen} and λ, where photon entropy, $\hat{S}_{\text{photon}}$, is the finite value suggested by Kirwan (2004). A three-dimensional plot or a contour plot can visually describe this relationship. In the case where photon entropy is considered zero, the equation is greatly simplified to:

$$Q = TS_{\text{gen}} + \Delta G_{\text{process}} - \Delta H_{\text{process}}$$

In this case, the heat rejected from the system is a function only of the internal entropy generated by the photosynthetic system, and a linear relationship can be observed.

Appendix B

Heat Transfer Profile for a Microalgae Species

B.1 Introduction

A heat transfer model for a microalgal species is approachable, due to its uncomplicated geometry, as one reason. A major microalgal species such as *Chlorella* exists as a collection of spherical cells of uniform composition surrounded by a water medium (Graham and Wilcox, 2000). Thus, with the knowledge that the species is unicellular, a model for one cell can be assumed to represent all the cells in the system. Again, the ongoing assumption is in place that biomass and algae cells in this case are approximated wholly as glucose.

The objective of developing a heat transfer model here is to obtain a temperature profile in order to observe whether or not the amount or rate of heat rejection by a cell is reasonable. By Fourier's law, a temperature gradient typically exists from one point to another where heat is rejected over an area in a material with a set or variable thermal conductivity. Figure B.1.1 indicates a proposed and simplified illustration of how the heat rejection over an algae cell might occur, based on work by (Bird et al., 2002) regarding heat rejection from a sphere in a stagnant fluid.

Heat transfer, in this case, happens in two concurrent stages. Firstly, heat transfer through a section of glucose or cellulose occurs from the inner core of the cell at temperature T_{i} to the surface of the cell with temperature T_{s}. Then, heat transfer occurs across a film of water from the surface of the cell to the bulk fluid of water. The cell has a radius R and the water has an ambient temperature of $T_{\mathrm{a}} = 25\,^{\circ}\mathrm{C}$, which is recognised as an effective temperature to

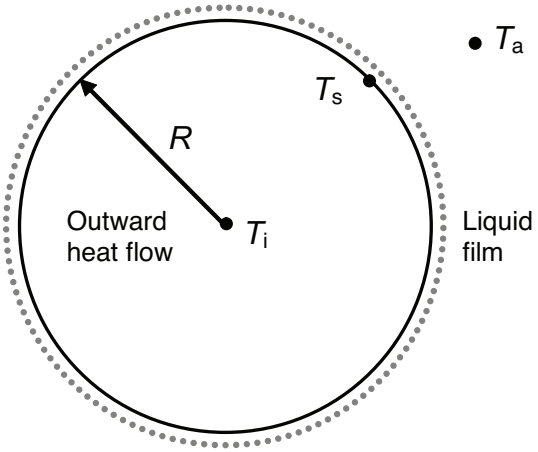


Figure B.1.1: Heat transfer over a simplified, spherical algal cell. Heat transfer occurs in the direction outwards from the centre of the cell, as well as over the surface of the cell to the bulk fluid (water) over a film of the fluid.

maximise algae growth (Burlew, 1953).

It is necessary before continuing here, to differentiate between specific forms of heat loss or rejection. Q is defined in this work is the heat rejected to the surroundings per mole of reaction of glucose or biomass formed, and thus has units of kJ/mol. In the case now of establishing a heat transfer model, the rate of heat transfer or energy rejected per time will be applied as symbol q and having units of W.

Over a period of time, one mole of algae, approximated as glucose and therefore having a mass of 180.16 g, will be grown with a total heat rejection rate of q_{total}. In order to determine what the rate of heat rejection across one cell (q_{cell}) in that mass of algae is, the number of cells must be calculated. This can be achieved by establishing a representative radius for these cells, and hence the volume of each cell, and then approximating the density of the algae a weighted average of glucose and water (1270 kg/m^3):

$$N_{\text{cells}} = \frac{180.16\ \text{g}}{\rho_{\text{average}} \left(\frac{4}{3}\pi R^3\right)}$$

With this knowledge, the total rate of heat rejection can be divided by the number of cells to determine the rate of heat rejection per cell:

$$q_{\text{cell}} = \frac{q_{\text{total}}}{N_{\text{cells}}}$$

Now, knowing what the rate of heat rejection per cell is, the model can begin to be developed. The assumption of steady state heat transfer is made

in order to simplify the model. In essence, it can describe the temperature profile across the cell as the algae grows and as heat from the excess incoming photons is rejected from the cell to the surrounding water. The primary aim is to observe how the inner core temperature differs from the ambient, bulk water temperature. If the cell is operating well above the ambient temperature, then this is an indication that the cell would be likely to be damaged and not able to reject heat at such a rate.

Comparison between the rates of heat rejection for the reversible case and the irreversible case will be made; the latter utilises the average literature requirement, while the former utilises the minimum limit of operation in terms of quantum requirement. Since heat rejected per mole of glucose formed by a photosynthetic organism, Q, is a function of incoming photon wavelength, λ, a set wavelength of 680 nm will be used, as this is a common absorbance peak for *chlorophyll a* (Berg et al., 2002). For the reversible process, the heat rejected is 233 kJ/mol of glucose produced from figure 2.2.4, and for the irreversible process this heat rejected is 8.05 MJ/mol of glucose produced, from figure 2.4.1.

B.2 Heat transfer over the cell

In order to describe the rate of heat released by the cell at any point in the spherical cell, a generation term, α, must be introduced. α represents the amount of energy per time generated per volume of the sphere (W/m^3). It is defined such that the rate of heat generated at the surface, where the sphere has a full radius of R, is equal to the rate of heat released by the cell:

$$\alpha = \frac{q_{\text{cell}}}{\frac{4}{3}\pi R^3} \tag{B.2.1}$$

To demonstrate the numerical value of α, consider the aforementioned heat rejection per mole of glucose produced for the reversible and irreversible processes using photons of wavelength 680 nm. Choosing a particle or radius size for a cell, it is possible to determine the number of cells, N_{cells}, and thus the heat rejected per cell, q_{cell}. Therefore, for a cell of 6 microns in radius, α will have a value of 1.65×10^9 W/m^3 and 5.67×10^{10} W/m^3 for the reversible and irreversible processes, respectively.

To describe the temperature and heat transfer profiles over a section of the cell, a steady state energy balance over a slice of the cell of thickness Δr can

be considered and mathematically described as:

$$q\mid_{r+\triangle r} = q\mid_r + (\alpha V\mid_{r+\Delta r} - \alpha V\mid_r)$$

What is being described here is essentially the following: the rate of heat transfer at $r+\Delta r$ is equal to the rate of heat transfer at r and the heat released or generated during Δr. This expands to:

$$q\mid_{r+\triangle r} - q\mid_r = \frac{4}{3}\pi\alpha\left[(r+\triangle r)^3 - (r)^3\right]$$

If the equation is further rearranged it arrives in this form, where the limit of this equation can be determined as $\Delta r \to 0$:

$$\lim_{\Delta r\to 0}\frac{q\mid_{r+\triangle r} - q\mid_r}{\Delta r} = \lim_{\Delta r\to 0}\frac{4}{3}\pi\alpha\left(3r^2 + 3r\triangle r + \Delta r^2\right)$$

The following differential equation is produced:

$$\frac{dq}{dr} = 4\pi\alpha r^2$$

Rearranging and integrating:

$$\int dq = 4\pi\alpha\int r^2.dr$$

$$q = \frac{4}{3}\pi\alpha r^3 + C_1$$

Here, C_1 is an arbitrary constant from the integration. It can be solved by considering the following condition: at the centre of the cell ($r = 0$), the rate of heat transfer is equal to zero. This is the case as the rate of heat transfer is a function of the heat generated, α, within the cell, which in turn is a function of volume. At the centre of the cell, the volume is zero, and therefore the rate of heat transfer is zero:

$$\text{At } r = 0,\ q = 0$$

$$\therefore C_1 = 0$$

Returning to the main equation, the rate of heat transfer at any point in the cell can thus be described as:

$$q = \frac{4}{3}\pi\alpha r^3$$

The rate of heat transfer, q, is therefore a cubic expression dependent on radius, with its maximum at the surface of the cell: q_{cell}. With this established, attention can now be turned to developing the temperature profile inside the cell. Fourier's law can be defined, for a sphere, as:

$$q = -k_{\text{cell}} \left(4\pi r^2\right) \frac{dT}{dr}$$

Here, k_{cell} is the thermal conductivity of the cell material, which can be approximated as that of glucose, cellulose or a similar biomass component. A thermal conductivity value of $0.4\,\text{W/m}^2\text{.C}$ for wood at $25\,^{\circ}\text{C}$ was chosen as an adequate approximation for this purpose. Equating this expression with the one above produces:

$$-k_{\text{cell}} \left(4\pi r^2\right) \frac{dT}{dr} = \frac{4}{3}\pi\alpha r^3$$

This can be simplified, rearranged and then integrated from the inner core temperature, T_{i}, at $r = 0$, to the surface cell temperature, T_{s}, at $r = R$:

$$\int_{T_{\text{i}}}^{T_{\text{s}}} dT = -\frac{\alpha}{3k_{\text{cell}}} \int_0^R r.dr$$

The final result indicates the temperature difference between the inner core and the surface of the spherical cell:

$$T_{\text{i}} - T_{\text{s}} = \frac{\alpha R^2}{6k_{\text{cell}}}$$

B.3 Heat transfer over the water film

With the temperature profile over the physical cell developed, attention must now be paid to describing the heat transfer from the surface of the cell to the surrounding water over a film of water. Applying Fourier's law to the case of a sphere with heat transfer from the surface to bulk fluid via a film:

$$q_{\text{cell}} = h_{\text{water}}(4\pi R^2)(T_{\text{s}} - T_{\text{a}})$$

Here, h_{water} is the film transfer coefficient for water. In order to determine its value, a correlation between it and a known quantity such as its thermal conductivity, k_{water}, which has a value of $0.611\text{W/m}^2\text{.C}$ at 25°C, must be made. The Nusselt number allows this very correlation to be made as a function of

cell radius R:

$$Nu = \frac{2hR}{k}$$

Bird et al. (2002) state that for heat transfer from a sphere to a stagnant fluid, the Nusselt number has a value of 2:

$$h_{\text{water}} = \frac{k_{\text{water}}}{R}$$

Thus, the heat transfer across the film can be represented as a function of α:

$$\frac{4}{3}\pi\alpha R^3 = (4\pi R^2)h_{\text{water}}(T_{\text{s}} - T_{\text{a}})$$

$$T_{\text{s}} - T_{\text{a}} = \frac{\alpha R}{3h_{\text{water}}}$$

If this equation is added to the resultant equation describing the temperature difference between the inner core of the cell and the surface, a full temperature profile from the inner cell core to the bulk water or ambient surroundings can be determined:

$$T_{\text{i}} - T_{\text{a}} = \frac{\alpha R}{3}\left(\frac{R}{2k_{\text{cell}}} + \frac{1}{h_{\text{water}}}\right)$$

The above equation is the final result of this section. It is capable of describing the inner core temperature of spherical microalgal cells of different radii, and with different rates of heats released to the surrounding water from the correlation between α and q_{cell}. A graph showing this relationship for the different rates of heat rejected by the aforementioned reversible and irreversible processes with incoming photons at 680 nm is shown as figure 2.4.3 in section 2.4 as part of the main dissertation text, where it is discussed.